REPORT No. 562

AIR FLOW IN THE BOUNDARY LAYER NEAR A PLATE

By HUGH L. DRYDEN

SUMMARY

The published data on the distribution of speed near a thin flat plate with sharp leading edge placed parallel to the flow (skin friction plate) are reviewed and the results of some additional measurements are described. These experiments were carried out at the National Bureau of Standards with the cooperation and financial assistance of the National Advisory Committee for Aeronautics for the purpose of studying the basic phenomena of boundary-layer flow under simple conditions.

When the distribution of mean speed is measured in a stream without pressure gradient, it is found that the flow for some distance from the leading edge corresponds to that derived theoretically by Blasius from Prandtl's equations for laminar flow. At a definite value of the Reynolds Number formed from the distance to the leading edge and the speed of the stream at a considerable distance from the plate, the flow departs from the Blasius distribution and after a long transition region has the characteristics of fully developed turbulent flow, hereinafter designated "eddying flow." The Reynolds Number at which transition occurs is a function of the initial turbulence of the air stream, decreasing as the turbulence is increased.

Small pressure gradients in the air stream greatly change the critical Reynolds Number for a given turbulence.

From measurements of the amplitude of the u-fluctuation of speed it was found that the laminar region exhibits comparatively large fluctuations induced by the turbulence of the general flow. The laminar and eddying regions cannot be distinguished on the basis of the magnitude of the speed fluctuation, but the principal fluctuations in the eddying region are of higher frequency than those occurring in the laminar region.

INTRODUCTION

It is becoming increasingly evident that the solution of problems of great importance to aircraft designers, especially the influence of Reynolds Number or scale effect and the influence of initial turbulence, demands a more complete knowledge of the flow near surfaces, that is, in boundary layers. Even in the simple case of boundary-layer flow near a skin-friction plate, i. e., a thin flat plate of great length and width placed parallel to the flow, our knowledge is far from complete. Studies of this simplified case are much needed to discover the basic laws of boundary-layer flow and thereby to prepare the way for a better understanding of the flow mechanism in the many cases of interest to the designer.

The concept of the boundary layer and the equations describing the laminar flow within it were announced by Prandtl in 1904 (reference 1). Four years later Blasius (reference 2) gave the solution of these equations for the skin-friction plate. A general acceptance of the boundary-layer concept was delayed for 20 years until experimental technique advanced to the point where the inner structure of the boundary layer could be explored in detail. The pioneer measurements were made by Burgers and his assistant, van der Hegge Zijnen, at Delft in 1924 (reference 3) with the aid of a hot-wire anemometer. Further measurements with pitot tubes were made a few years later by Hansen (reference 4) and by Éliás (reference 5) at Aachen. Later developments have shown that the comparatively good agreement between the results at Delft and Aachen was somewhat fortuitous. It seemed worth while to make some further measurements in an air stream of considerably smaller turbulence and, in view of the development of equipment for measuring the velocity fluctuations parallel to the mean direction of flow, to study the fluctuations as well as the mean speed.

The primary interest in this work is in the field of flow (distribution of speed in the vicinity of the plate), and not in the skin friction itself, which is more easily studied by force measurements. Th. von Kármán has recently (reference 6) given a review of the data on skin friction.

ACKNOWLEDGMENT

The author wishes to acknowledge the assistance of A. M. Kuethe, W. C. Mock, Jr., and S. S. West in connection with the experimental program and the reduction of observations; of W. H. Boyd in the design and construction of the traversing equipment; and of E. R. Frisby in the computation of the effect of the "simplified turbulence."

PREVIOUS EXPERIMENTAL WORK

The essential features of the flow in the boundary layer of a skin-friction plate may be described by a consideration of the measurements of Burgers and van der Hegge Zijnen (reference 3). The results are presented in the dissertation of van der Hegge Zijnen in the form of numerous tables and curves giving the observed speeds at several hundred points, whose x and y coordinates with respect to the leading edge of the plate are tabulated, for five speeds of the approaching air stream. The original dissertation should be consulted for detailed results. Only the general features can be discussed here.

Dimensional analysis enables one to devise a method of representation that gives a general view of the hundreds of measurements. The speed u at any point (x, y) at distance x from the leading edge and at distance y from the plate is a function of the speed U_0 of the approaching air stream, of the density ρ and the viscosity μ of the air, and of x and y. By the principles of dimensional analysis

$$\frac{u}{U_0}=f\left(\frac{U_0 x}{\nu},\frac{U_0 y}{\nu}\right) \qquad (1)$$

where ν is the kinematic viscosity μ/ρ. The independent variables may be considered as x-Reynolds Number and y-Reynolds Number, since a nondimensional product obtained by multiplying $\frac{U_0}{\nu}$ by a linear dimension is ordinarily called a "Reynolds Number." If the foregoing factors are the only ones determining the flow, the flow can be pictured by a three-dimensional model or, more conveniently, by a contour diagram of the three-dimensional model. This representation is entirely independent of any theory of the flow and its validity rests only on the completeness of the list of controlling quantities.

A contour diagram of this type for the measurements of van der Hegge Zijnen is given in figure 1. The contours are for values of u/U_0 in steps of 0.1, the corresponding x and y being found by interpolation in the original tables. For convenience, the scale of y-Reynolds Number has been magnified 200 times. If one wishes to think in terms of x and y, the numbers along the abscissas represent for an air speed of 200 feet per second distances in inches, while each square along the ordinates represents one one-thousandth of an inch. Or for an air speed of 20 feet per second, the numbers along the abscissas are tens of inches and each square along the ordinates is one one-hundredth of an inch.

The diagram contains data for five speeds and, in general, the results are very consistent. The deviations correspond to about 0.02 in u/U_0 or 0.005 inch on the average in y. When examined on a large scale there are certain systematic differences between the results at different speeds, which are to be ascribed to the influence of a slight pressure gradient in the air stream in which the measurements were made.

Near the leading edge the contour lines are approximately parabolic in shape and correspond approximately to the theoretical result of Blasius for laminar flow (cf. theoretical treatment). For this reason, the flow in this part of the field is labeled "laminar."

At an x-Reynolds Number of about 300,000, the contours for small values of u/U_0 approach the axis of abscissas, indicating an increasing speed along the plate while the contours for large values bend away from the axis, indicating a rapid thickening of the layer. The process continues over the range from 300,000 to about 500,000, a region usually designated as the "transition" region.

There follows a different type of speed distribution which resembles very closely that found in eddying (fully developed turbulent) flow in pipes. In the part marked "eddying layer," there is at any x-Reynolds Number, a logarithmic relation between u and the y-Reynolds Number, often approximated by a power law. The relations are different near the wall, a region commonly termed the "laminar sublayer" because the distribution resembles that in the laminar layer. It should be noted that the laminar sublayer accounts for only a small part of the thickness of the layer but for two-thirds of the fall in speed.

The contour for $\frac{u}{U_0}=1$ is not shown, for the reason that u approaches U_0 asymptotically. Various unambiguous procedures can be used to define the "thickness" of the layer of fluid affected by the presence of the plate. We may perhaps think of the distribution as approximated by some specific mathematical expression, and the thickness δ as the value of y which, substituted in that expression, gives $u=U_0$. Or δ may be taken as the value of y, for which $u=0.99\ U_0$ or $0.995\ U_0$ or some other convenient value. The "displacement thickness" δ^* defined as $\int_0^\infty\left(1-\frac{u}{U_0}\right)dy$ is often the most convenient measure of the thickness.

Burgers and van der Hegge Zijnen made another significant observation, namely, that the presence of strong fluctuations in the flow of air approaching the plate moved the transition to an x-Reynolds Number of about 85,000. The fluctuations were produced by a square-mesh wire screen immediately ahead of the plate, the wire diameter being 0.08 cm and the mesh being 0.4 cm.

In air streams, especially those produced by artificial means in wind tunnels, the motion is never absolutely steady, and there are always present small ripples or fluctuations that usually do not exceed a few percent of the average speed. It is difficult to believe that the presence of these fluctuations, usually of frequencies of the order of 20 to perhaps 1,000 per second, could play any part in determining the nature of the flow around an object placed in the stream. Yet it has been experimentally found that these fluctuations

exert a comparatively large influence in many cases. The basic effect in all these cases is believed to be the effect on the transition from laminar to eddying flow in the boundary layer.

No method by which the initial turbulence could be numerically evaluated was known in 1924 and the methods are still in process of development. No completely satisfactory method can be developed until a satisfactory theory of the effect of turbulence is available. It is now possible to measure directly (reference 7) the mean fluctuation of the speed at any point with time by means of a hot-wire anemometer, with a wire of small diameter, an amplifier, an electrical network to compensate for the lag of the wire, and an alternating current milliammeter. The speed fluctuation is converted into an alternating electric current whose intensity is measured. The turbulence may then be defined as the ratio of the average fluctuation to the mean speed and is usually expressed as a percentage. Such a method was used in the experiments described in this paper.

Because of certain small discrepancies between the experimental results of van der Hegge Zijnen in the region of laminar flow near the leading edge and the theory of Blasius, the measurements were repeated by M. Hansen at Aachen (reference 4), using small pitot tubes. In general appearance, a contour diagram of the results would resemble figure 1. The data of Hansen are not given in sufficient detail to permit the preparation of an accurate contour diagram. The transition occurred at nearly the same value of the x-Reynolds Number, a fact which the experiments in the present paper show to be a coincidence. The principal differences between the two sets of measurements at Delft and Aachen are: (1) the Aachen results agree very well with the Blasius theory, whereas the Delft results show small discrepancies; and (2) when the speed distribution in the eddying region is approximated by a power law, the exponent is about 1/5 in the Aachen experiments as compared with 1/7 in the Delft experiments.

Hansen showed that the Delft experiments were made in an air stream in which the static pressure decreased along the plate and that therefore the experiments could not be expected to check the theory of Blasius, which assumed a constant static pressure along the plate. An approximate allowance for the effect of the pressure gradient brought the Delft experimental results into agreement with the Blasius theory.

Hansen made some studies of the effect of the shape of the leading edge of the plate and of the roughness of the surface. A poorly shaped leading edge sets up turbulence which has an effect similar to that of increased turbulence in the air stream. For rough plates, the flow was eddying at all points investigated.

Éliás (reference 5) also made measurements of the speed distribution near a plate in connection with measurements of heat transfer. The results are similar to those of Hansen and were presumably made in the same wind tunnel. Transition occurred at an x-Reynolds Number of about 150,000 to 200,000.

THEORETICAL TREATMENT

Laminar flow.—The equations given by Prandtl for the steady flow of an incompressible fluid in a thin boundary layer along a two-dimensional plane surface are as follows:

$$u\frac{\partial u}{\partial x}+v\frac{\partial u}{\partial y}=\nu\frac{\partial^2 u}{\partial y^2}-\frac{1}{\rho}\frac{\partial p}{\partial x} \tag{2}$$

$$\frac{\partial p}{\partial y}=0 \tag{3}$$

$$\frac{\partial u}{\partial x}+\frac{\partial v}{\partial y}=0 \tag{4}$$

where u is the component of the velocity parallel to the surface, v the normal component, x the distance measured along the surface, y the distance measured normal to the surface, ν the kinematic viscosity, and p the pressure. The boundary conditions are: (1) at the surface, $u=v=0$; (2) at a great distance $u=U$, the speed in the potential flow. By (3) the pressure is independent of y and hence equal to that in the potential flow. By Bernoulli's theorem $p+\frac{1}{2}\rho U^2$ is constant and hence, $\frac{\partial p}{\partial x}=\rho U\frac{dU}{dx}$.

Blasius discussed the case where U, the speed at a considerable distance from the plate, is constant, i. e., $\frac{dU}{dx}=0$ and therefore $\frac{\partial p}{\partial x}=0$. This constant value of U will be designated U_0.

By virtue of equation (4), a stream function ψ may be introduced, such that

$$u=-\frac{\partial \psi}{\partial y},\ v=\frac{\partial \psi}{\partial x} \tag{5}$$

Equation (2) becomes for $\frac{dp}{dx}=0$

$$-\frac{\partial \psi}{\partial y}\frac{\partial^2 \psi}{\partial x \partial y}+\frac{\partial \psi}{\partial x}\frac{\partial^2 \psi}{\partial y^2}=\nu\frac{\partial^3 \psi}{\partial y^3} \tag{6}$$

Introducing new variables [1] Z and X defined by

$$Z=\frac{1}{\sqrt[3]{\alpha}}\frac{\psi}{\sqrt{\nu U_0 x}},\ X=\frac{\sqrt[3]{\alpha}}{2}\sqrt{\frac{U_0}{\nu x}}y \tag{7}$$

in which α is a numerical constant whose significance and value will be determined later, equation (6) becomes

$$\frac{d^3 Z}{dX^3}+Z\frac{dZ}{dX}=0 \tag{8}$$

Setting $\bar{u}=\frac{u}{U_0}$ and $\bar{y}=y\sqrt{\frac{U_0}{\nu x}}$, it may be shown from (5) and (7) that

$$\bar{u}=\frac{\alpha^{2/3}}{2}\frac{dZ}{dX}\text{ and }\bar{y}=\frac{2}{\alpha^{1/3}}X \tag{9}$$

[1] In view of the more complete derivations published elsewhere, for example, reference 2, only the principal steps in the method of solution will be outlined.

Likewise

$$\frac{d\bar{u}}{d\bar{y}}=\frac{\alpha}{4}\frac{d^2Z}{dX^2} \text{ and } \frac{d^2\bar{u}}{d\bar{y}^2}=\frac{\alpha^{2/3}}{8}\frac{d^3Z}{dX^3} \quad (10)$$

The boundary conditions, $u=v=0$ at the surface and $u=U_0$ for large values of y become in the new variables

$$\frac{dZ}{dX}=0, Z=0 \text{ at } X=0 \text{ and } \frac{\alpha^{2/3}}{2}\frac{dZ}{dX}=1 \text{ at } X=\infty \quad (11)$$

In the solution of equation (8) it is convenient to begin the solution at the surface. By the introduction of the numerical constant α, the value of $\frac{d^2Z}{dX^2}$ at $X=0$ may be assumed equal to 1, this boundary condition temporarily replacing condition (11). When the solution has been obtained, α may then be chosen to satisfy (11). It may be noted that α does not appear in (8).

Equation (8) may be solved numerically by the Runge-Kutta method (reference 8). The results are given in table I. The value of α is found to be 1.328238. From this value and equations (9) and (10), $\bar{y}$, $\bar{u}$, $\frac{d\bar{u}}{d\bar{y}}$, and $\frac{d^2\bar{u}}{d\bar{y}^2}$ are readily computed. These quantities are also given in table I.

It is significant that the complete solution can be represented by a single curve of $\bar{u}$ plotted against $\bar{y}$. Thus the speed distributions at various values of x are similar, the same speed occurring at values of y proportional to the square root of $\frac{\nu x}{U_0}$. This similarity of the speed distributions is the physical expression of the reduction of the partial differential equation to a total differential equation. On the representation of the laminar speed distribution by a contour diagram similar to figure 1, it is readily seen that a constant value of $\bar{y}$ corresponding to a given $\bar{u}$ is indicated by a constant value of the ratio of the y-Reynolds Number to the square root of the x-Reynolds Number, which ratio numerically equals $\bar{y}$. Hence the contours are parabolas. The values of $\bar{y}$ at even values of $\bar{u}$ for the theoretical laminar distribution are given in the following table:

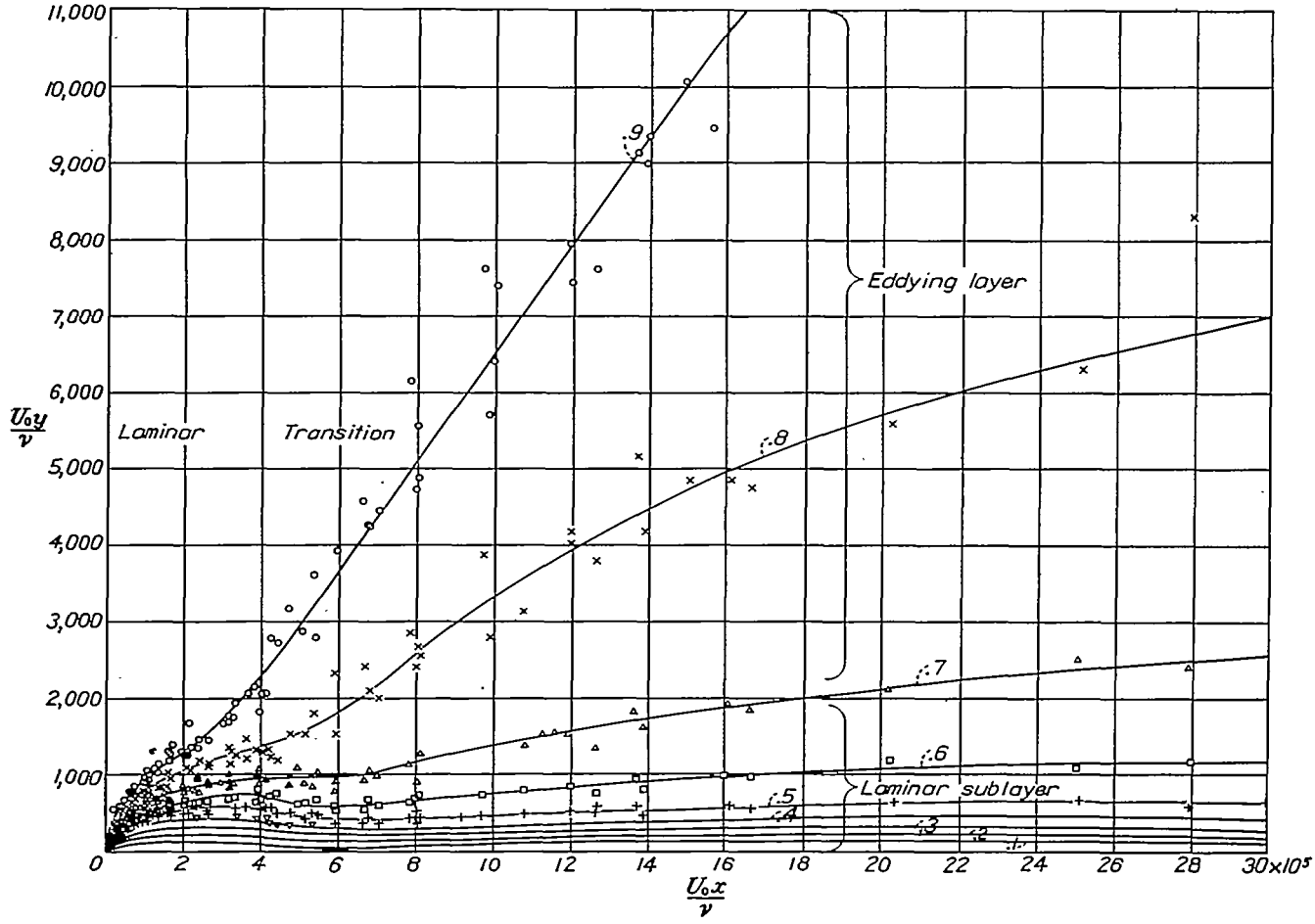

FIGURE 1.—Distribution of mean speed near skin-friction plate. Measurements made by van der Hegge Zijnen. x is the distance measured along the plate from the leading edge, y the distance from the plate, U_0 the speed of the free stream, ν the kinematic viscosity. The contours are contours of equal mean speed, the number on each contour being the corresponding value of u/U_0, where u is the local speed.

$\bar{u}$	$\bar{y}$	$\bar{u}$	$\bar{y}$
0.1	0.301	0.6	1.890
.2	.603	.7	2.276
.3	.908	.8	2.739
.4	1.220	.9	3.385
.5	1.544		

The equations of the contour lines are

$$\frac{U_0 y}{\nu}=\bar{y}\sqrt{\frac{U_0 x}{\nu}} \tag{12}$$

The "displacement thickness" δ^* is readily computed from table I to be $1.7207\sqrt{\frac{\nu x}{U_0}}$, and hence the δ^* Reynolds Number is 1.7207 times the square root of the x-Reynolds Number.

When a pressure gradient is present so that $\frac{dp}{dx}$ is not zero, the similarity of the speed distributions disappears except in special cases, and the partial differential equation must be solved. Various approximate methods have been proposed, for example, those described in references 9, 10, 11, and 12. For small pressure gradients with the pressure decreasing downstream, the computed effect on the contour diagram representation is to move the contours closer to the axis of abscissa, i. e., to decrease the rate of thickening of the boundary layer. The $\bar{u}$ or $\bar{y}$ curve is not independent of x; in general $\bar{u}$ increases with $\bar{y}$ more rapidly than for the Blasius case and approaches the asymptote to a given approximation at a smaller value of $\bar{y}$. The departure from the Blasius curve increases with increasing x. The effect of a small gradient is surprisingly large.[2] The references cited may be consulted for a detailed discussion.

Transition.—The physical factors that determine the transition from laminar to eddying flow are not clearly understood. The principal theoretical developments have proceeded from the assumption that the origin of eddying flow is to be sought in the instability of the laminar flow under certain circumstances. The difficult mathematical computations have been made by Tollmien (reference 13) and Schlichting (reference 14) of the Göttingen group for the following idealized case. A steady two-dimensional laminar flow is assumed in which the velocity depends only on the coordinate normal to the direction of flow. Small disturbances are superposed on this basic flow in the form of waves propagated in the direction of flow. These disturbances are assumed to satisfy the Navier-Stokes equations and the usual boundary conditions. It is then determined whether waves of any given frequency are damped or amplified.

In the computation it is found necessary, in order to obtain a *linear* differential equation, to assume the amplitude of the disturbances sufficiently small that only first-order terms need be retained. The viscosity effects are assumed small, zero in fact, except near the boundary and in a critical layer where the wave velocity of the disturbance equals the speed of the basic flow. If the viscosity were neglected everywhere, the amplitude of the disturbance would become infinite in this critical layer, thus invalidating the neglect of terms of higher order than the first.

The results obtained for the Blasius distribution of the preceding section as the basic flow are given in figure 2. The region marked "unstable" represents those values of Reynolds Number and wave length for which small disturbances are amplified. Disturbances for wave lengths and Reynolds Numbers outside that region are damped. The displacement thickness δ^* is used as the characteristic length in the Reynolds Number and as the unit for measuring the wave length.

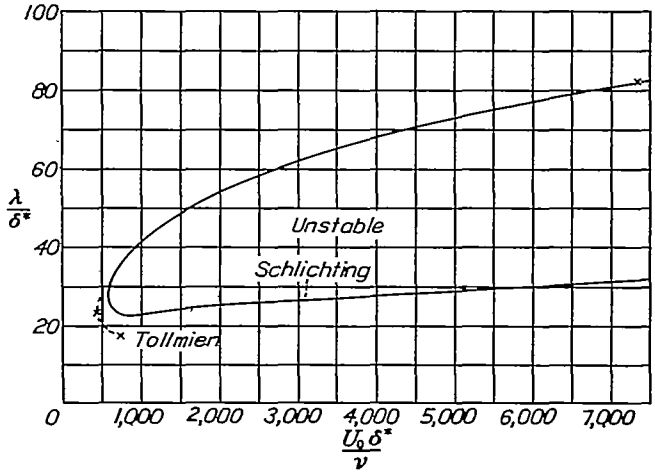

FIGURE 2.—Wave length of sinusoidal disturbances which produce instability of laminar flow near a plate according to Tollmien and Schlichting. λ is the wave length, δ^* is the displacement thickness of the boundary layer, U_0 the speed of the free stream, ν the kinematic viscosity.

Tollmien (reference 15) has shown that velocity distributions having an inflection point, which occur in boundary layers when the pressure increases downstream, are unstable and that the amplification of small disturbances is of a higher order of magnitude than the one found for the Blasius distribution. Thus the nondimensional amplification factor is of the order of 0 to 0.05 for the distribution with inflection point as compared with 0 to 0.007 for the Blasius distribution.

These theoretical calculations are of the utmost importance in the study of the origin of eddying flow. The amplified disturbances do not, however, in themselves constitute eddying flow. The wave lengths of the amplified disturbances are of the order of 25 to 50 or more times the displacement thickness. Schlichting (reference 14) computed the maximum possible amplification of the disturbances and concluded that a fourfold to ninefold amplification appeared sufficient to produce eddying flow from the long-wave disturbances as judged by a comparison of experimentally observed transition points with the theoretically computed maximum amplification in passing along the plate to the

[2] See also page 344.

observed transition point. It appears to be the opinion of Tollmien that the formation of velocity distributions with inflection points constitutes an intermediate step in the development of eddying flow, these distributions arising as the long-wave length disturbance increases in amplitude.

An attempt was made by Nikuradse (reference 16) to check the theory. A glass plate with a faired leading edge of metal was set up in a water channel provided with slightly diverging walls to give constant static pressure along the plate. The disturbances in the flow were reduced as much as possible, giving a transition at an x-Reynolds Number of 655,000 or a δ^*-Reynolds Number of 1,400. Artificial disturbances of approximately sinusoidal character and of varying frequency were produced by a varying suction applied to holes in the faired leading-edge strip. Except for three points at very low frequency, transition occurred at a δ^*-Reynolds Number between 790 and 1,050, the majority of the points scattering about a value of 850. There was no indication that the frequency of the disturbance had any marked effect as would be inferred from the computations of Tollmien and Schlichting. Nikuradse states, "Perhaps the explanation is that, since the disturbance impressed on the boundary layer is not of perfectly sinusoidal form, some harmonic of the disturbance acts to produce turbulence. A clear decision for or against the Tollmien theory is accordingly still lacking."

In the opinion of the author the numerous experiments on the critical Reynolds Number of spheres and airship models in relation to measurements of the fluctuations present in the air stream furnish additional evidence that it is the amplitude of the disturbances initially present rather than their frequency which is of primary importance and, as in Nikuradse's experiments, if the amplitude is fixed, the point of transition is but little affected by the frequency, provided the frequency is not too low.[3]

The theory of small vibrations in which only first-order terms are retained cannot give any information as to the influence of amplitude of the fluctuations originally present in the flow. In reference 17 the author outlined briefly the following conception of the mechanism of transition:

> The observed fluctuations of speed at a fixed point may be taken as an indication that at any one time there are variations of speed along the outer edge of the boundary layer. With the speed variations there will be associated variations of pressure, and in the regions where the speed is decreasing, the pressure will be increasing. The magnitude of the pressure gradient depends on the amplitude and frequency of the speed fluctuations, increasing as either increases. At a sufficient distance from the leading edge, the thickness of the boundary layer will be such that there will be a reversal of the direction of flow near the surface in those places where the pressure is increasing downstream. Larger speed fluctuations bring larger pressure gradients and an earlier reversal of flow. It seems very probable that such a reversal would give rise to the formation of eddies.

This conception differs from that of Tollmien in that (1) the disturbances are "forced" by the external turbulence rather than being "free vibrations" and (2) the eddying flow is assumed to originate in velocity distributions with reversed flow which occur as a result of separation rather than in distributions which have only inflection points.

Some computations have been made to show the sensitivity of a boundary layer to small pressure gradients and the facility with which separation occurs. The computations were made by a modification of Pohlhausen's method, which has been described in reference 11. The problem treated was that of the laminar boundary layer of a plate in a steady external flow

$$\frac{U}{U_0}=1+0.02 \sin\left(2\pi\frac{X}{\lambda}-\alpha\right)$$

In other words, a sinusoidal variation (with distance x) of amplitude equal to 2 percent of the mean speed, wave length λ, and phase α relative to the leading edge of the plate was superposed on the uniform flow of speed U_0. Computations were made for ten values of α corresponding to displacement of the sine wave by steps of 0.1 λ. The speed distributions obtained for two values of α are shown in figure 3. Separation occurs at the points indicated.

Each of these computations refers to a steady flow, the distribution being independent of the time. As a rough approximation to a traveling wave we may, however, consider the sine wave slowly displaced along the plate and inquire as to the value of the mean speed at a given point and of the variation of the speed at that point. The mean speed is found to be practically identical with the Blasius distribution. The speed fluctuations expressed as root-mean-square values are plotted in figure 4.

The essential features of the results to which we shall have occasion to refer are as follows:

1. The mean speed is practically unaffected by this simplified turbulence of the external flow.

2. There are speed variations within the boundary layer which are much larger than those in the external flow. Their amplitude increases with distance from the leading edge of the plate.

3. The point of separation is not fixed but moves back and forth within certain limits.

4. The position of the separation point and the distribution of the speed variations depend on the wave length λ.

5. While computations for only one amplitude have been made in full, it may be shown that there is a marked dependence of the location of the separation point on the amplitude of the speed variation in the external flow.

[3] It is known that there is some effect of "average size of eddies" on the critical Reynolds Number of a sphere, but the effect is of a lower order of magnitude than the effect of amplitude of the speed fluctuation.

The variation of speed in the external flow along the plate at any given instant is not sinusoidal in character, and it is not at all evident that the quasi-stationary method of computation is justified. All the results listed, however, are in agreement with experimental data except 4, the effect of wave length. The two theories of the transition are, in a sense, supplementary. If the fluctuations are extremely small, eddying flow may arise in the Tollmien manner from accidental disturbances. If the fluctuations are sufficiently large,

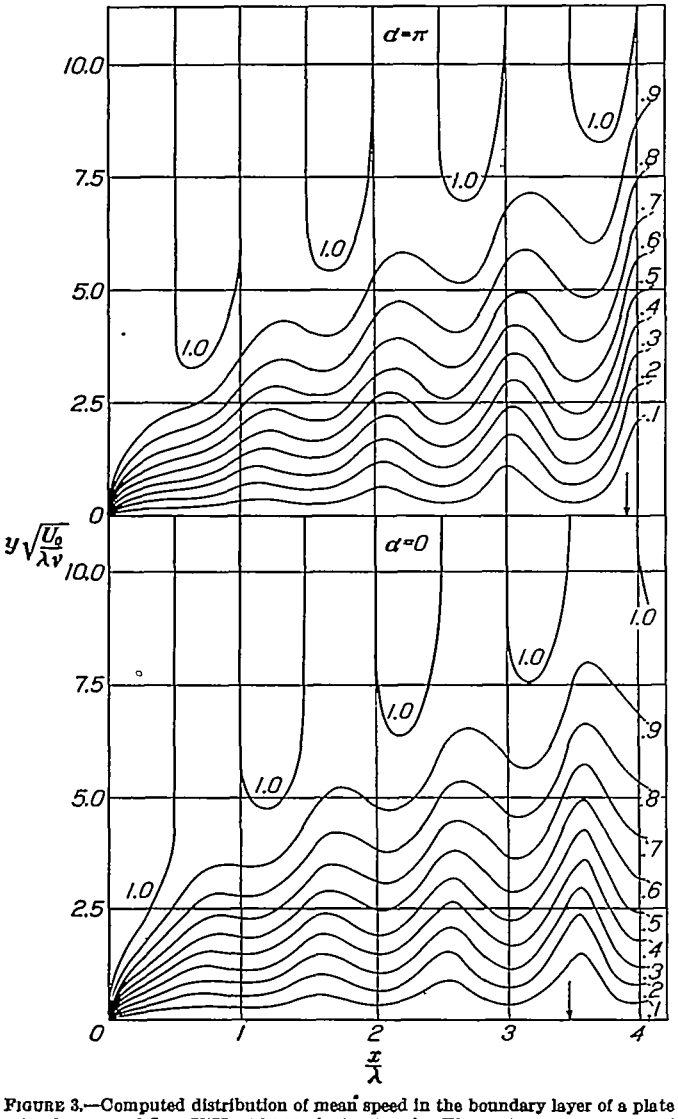

FIGURE 3.—Computed distribution of mean speed in the boundary layer of a plate for the external flow $U/U_0=1+0.02\sin(2\pi x/\lambda-\alpha)$. The contours are contours of equal values of u/U_0. Separation begins at the points indicated by arrows.

as probably happens in most practical cases, the eddying flow arises from the forced fluctuations of the boundary layer. The two pictures agree in exhibiting fluctuations of wave lengths that are long as compared with the thickness of the boundary layer. These fluctuations produce pressure gradients as a preliminary step. The long-wave disturbances do not themselves constitute eddying flow, although they involve comparatively large speed fluctuations. The correctness of either picture must be left an open question in view of the large effect of frequency required by both, which was not found in Nikuradse's experiments.

Eddying flow.—In experimental work on eddying flow, the distribution of mean speed near a wall is found to be represented fairly well by a power law of the form $u=ay^n$, where u is the mean speed, y the distance from the wall, and a and n are empirical constants. For Reynolds Numbers that are not too large, n is approximately 1/7 and this value has been much used as the starting point in computing the friction.

This purely empirical representation has been superseded by a formula having some theoretical backing, namely,

$$u=\left(\frac{\tau_0}{\rho}\right)^{1/2}\left[a+\frac{1}{k}\log\left(\frac{\tau_0}{\rho}\right)^{1/2}\frac{y}{\nu}\right] \qquad (13)$$

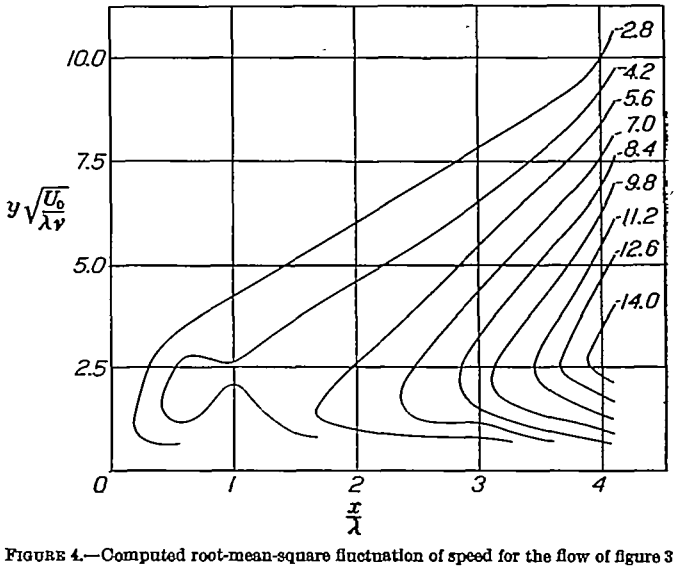

FIGURE 4.—Computed root-mean-square fluctuation of speed for the flow of figure 3 when α is varied from 0 to 2π. The contours are contours of equal values of the root-mean-square u-fluctuation expressed in percent of the speed of the free stream. In the free stream the fluctuation is 1.4 percent of the mean speed.

where τ_0 is the shearing stress at the wall, ρ is the density of the fluid, ν the kinematic viscosity, and a and k are constants. This equation is due to von Kármán. (See reference 6.)

The original paper should be consulted for a detailed discussion of the theory. The formula is derived for the idealized case of a *constant* shearing stress transferred in parallel flow along a wall. Both in a pipe and near a wall, the shearing stress is not constant but decreases with increasing distance from the wall. Nevertheless the formula is found experimentally to fit the velocity distribution as far as the center of the tube or the outer edge of the boundary layer, and the constant k is nearly the same whether computed from velocity distribution in smooth or rough pipes or near a wall, or from skin-friction measurements in smooth or rough pipes or on plates.

For the case of the skin-friction plate, it is convenient to set $\frac{2\tau_0}{\rho U_0^2}=c_f$, the local friction coefficient,

and to write equation (13) in the form

$$\frac{u}{U_0}=\left(\frac{c_f}{2}\right)^{1/2}\left[a+\left(\frac{1}{k}\right)\log\left(\frac{c_f}{2}\right)^{1/2}\left(\frac{U_0 y}{\nu}\right)\right] \quad (14)$$

Then setting $y=\delta$ for $\frac{u}{U_0}=1$ and subtracting the resulting equation from (14), we find

$$\frac{u}{U_0}-1=\frac{(c_f/2)^{1/2}}{k}\log\frac{y}{\delta} \quad (15)$$

In order to show the similarity with the power-law formula, (15) may be written

$$e^{\frac{u}{U_0}-1}=\left(\frac{y}{\delta}\right)^{\frac{(c_f/2)^{1/2}}{k}} \quad (16)$$

For small values of $\frac{u}{U_0}-1$, the term on the left may be expanded in the series $1+\left(\frac{u}{U_0}-1\right)+\frac{1}{2}\left(\frac{u}{U_0}-1\right)^2$ etc., whence, retaining only the first two terms

$$\frac{u}{U_0}=\left(\frac{y}{\delta}\right)^{\frac{(c_f/2)^{1/2}}{k}} \quad (17$$

Thus the exponent in the empirical power law representation may be expected to be a function of the local friction coefficient, and the power law representation itself may be expected to be valid only for small values of $\frac{u}{U_0}-1$.

The velocity distribution in the laminar sublayer near the wall may be approximated by solving the equation $\tau_0=\mu\frac{du}{dy}$, assuming τ_0 constant. The result is

$$u=\frac{\tau_0}{\rho}\frac{y}{\nu} \text{ or } \frac{u}{U_0}=\frac{c_f}{2}\frac{U_0 y}{\nu} \quad (18)$$

From von Kármán's universal velocity distribution near a smooth wall, which was based on the data of Nikuradse, the transition between (18) and (14) extends from $(c_f/2)^{1/2}\frac{U_0 y}{\nu}=8$ to $(c_f/2)^{1/2}\frac{U_0 y}{\nu}=100$. For $c_f=0.01$, the range of $\frac{U_0 y}{\nu}$ is from 113 to 1,413; for $c_f=0.001$, the range is from 358 to 4,473. Hence (14) cannot be expected to hold accurately for $\frac{U_0 y}{\nu}<$ about 4,000.

MEASUREMENTS AT THE NATIONAL BUREAU OF STANDARDS

APPARATUS

Wind tunnel.—The measurements were made in the 3-foot wind tunnel of the National Bureau of Standards from December 1929 to November 1930. A sketch of the tunnel and a brief description are given in reference 18. The tunnel is of the room return type with closed cylindrical working section, 6 feet long and 3 feet in diameter. The area of the entrance cross section, at which the honeycomb is located, is 5.44 times the working cross section. The turbulence at the working section is 0.5 percent, the critical Reynolds Number for a 5-inch sphere being 270,000.

The plate.—Two plates were used in the course of the work. Each was a polished aluminum plate, ⅛ inch thick and 2 feet wide. In the preliminary series of measurements, the plate was 49 inches long and the leading edge was beveled as indicated at E in figure 5. Since the preliminary measurements indicated a considerable disturbance at the leading edge, this plate was discarded. A new plate, 60 inches long, with leading edge sharp and symmetrically shaped as shown at E in figure 6 was used for all other measurements.

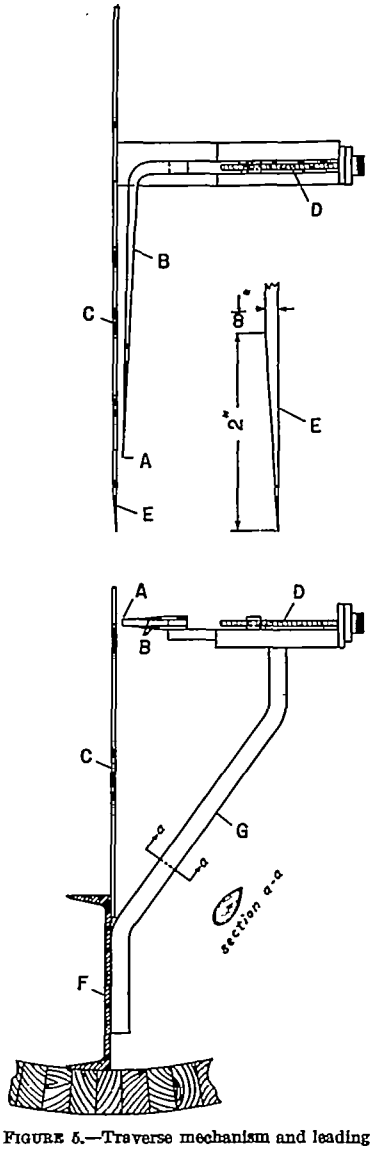

FIGURE 5.—Traverse mechanism and leading edge shape used in the preliminary measurements (series A).

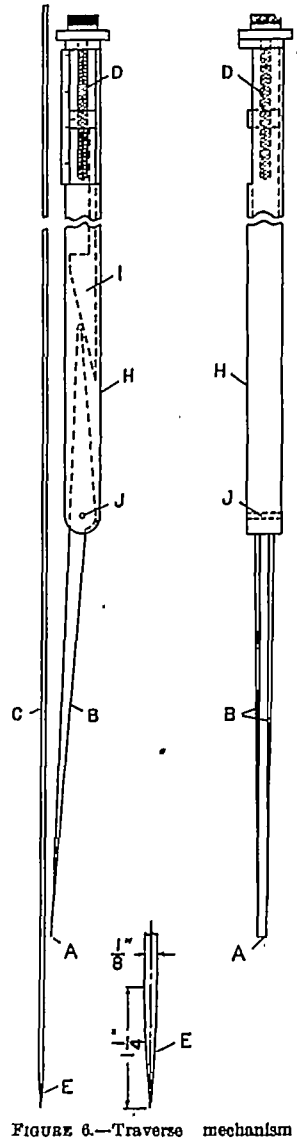

FIGURE 6.—Traverse mechanism and leading edge shape used in the later measurements (series B, C, and D).

The plate was mounted on two light 7-inch channels as shown at F in figure 5. The channels ran longitudinally parallel to the axis of the wind tunnel, one flange of each channel being fastened to the tunnel wall. The webs furnished supports for the edges of the plate and filled the gap between the edges of the plate and the tunnel wall.

The upstream edge of the plate was approximately 2 feet downstream from the upstream end of the working section and the downstream edge was within the expanding exit cone.

The hot-wire anemometer.—The speeds were measured by a hot-wire anemometer and associated equipment. The wire used was a platinum wire 0.017 mm in diameter and about 8 mm long. This very small wire was used to permit measurements of rapid fluctuations in speed as well as the mean speed.

In the preliminary series of measurements, the mounting shown in figure 5 was used. The wire A was mounted at the ends of the prongs B which ran downstream from the wire for about 12 inches. The prongs were bent at right angles and supported on a movable slide, which in turn was supported from the lower channel F by the bent streamline bracket G. The position of the wire relative to the plate C was varied by means of the micrometer screw D. The reading of the screw for zero distance was determined either by moving the wire in until the prongs touched the plate as determined by an auxiliary electric circuit or, better, by observing the reflection of the wire in the mirror surface of the plate. When observing the reflection, the mounting could be adjusted by shimming the bracket until the wire was accurately parallel to the plate.

Since the wire expands when heated and contracts when cooled, the prongs must be flexible. Otherwise a wire which is taut and straight when cool will become slack when heated or, if adjusted when heated, it will break when the heating current is shut off. Satisfactory results were obtained by using fine steel needles for the extreme tips. The fine platinum wire was electrically welded to the needles.

The long bracket G of this mounting tended to vibrate at high wind speeds, making the distances of the wire from the plate uncertain and a small but measurable effect on the static pressure at the position of the wire was detected. The slide and bracket block an undesirably large percentage of the area of the air stream. Hence when the preliminary measurements were completed, a new and improved mounting was constructed.

The improved mounting (fig. 6) was contained wholly within a tube H having a cross section about 1 inch square. The axis of the tube was parallel to the air flow and the tube was clamped directly to the plate with small spacing blocks between the tube and the plate. The wire prongs were rotated about the fulcrum J (fig. 6) by the cam I, which was moved by the micrometer screw D. The wire was 13.28 inches from the fulcrum, so that for small lateral displacements the wire moved practically at right angles to the plate. The micrometer screw was calibrated in terms of lateral movement of the wire in an auxiliary apparatus in which the lateral displacement was measured by means of a second micrometer screw.

The improved mounting showed no observable effect on the static pressure at the wire position and the blocking was inappreciable. The vibration of the wire relative to the plate was greatly reduced. There is perhaps some slight deflection of the prongs at high wind speeds because of wind pressure on the prongs.

The associated equipment is essentially as described in the appendix to reference 18. The fundamental theory of the hot-wire anemometer as used for measuring mean speed and fluctuations in the mean speed is given in reference 7. The performance of the particular equipment used in these measurements as regards accuracy of compensation for the lag of the wire is given in figure 1 of reference 17. The measurements were completed before the development of the improved equipment described in reference 19.

REDUCTION OF OBSERVATIONS

At a given distance from the front edge of the plate and for a given speed, the following observations were made:

1. Micrometer reading for $y=0$.
2. Voltage of potentiometer battery (by comparison with standard cell).
3. Resistance of wire at air temperature.
4. Voltage drop across wire for various air speeds with wire about 1 inch from plate (i. e., in free air stream).
5. For 10 or 15 values of y, values of the average voltage drop and the root-mean-square voltage fluctuation. The average current through the wire was adjusted to be 0.2 ampere at each value of y. The resistance to be used in the compensation circuit of the amplifier was computed and the adjustment made at each value of y. The amplifier was calibrated before and after the series.
6. Items 1, 2, 3, 4 were repeated in reverse order.
7. Frequent observations were made of air temperature, and the barometric pressure was read at the beginning and end of the series.

Calibration of the wire.—The relationship between the heat loss H and the speed u is given by the formula

$$H=(A+B\sqrt{u})\theta \tag{19}$$

where θ is the difference in temperature between the wire and the air and A and B are constants for a given wire. If i is the heating current and R the resistance of the heated wire (exclusive of the leads) when exposed to the stream, $H=i^2R$. Denoting the resistance of the wire at air temperature by R_0 and the temperature coefficient of resistance referred to that temperature by α

$$\theta=\frac{R-R_0}{R_0\alpha} \tag{20}$$

Thus the calibration formula (19) may be written in the form

$$\frac{H}{\theta}=\frac{i^2RR_0\alpha}{R-R_0}=A+B\sqrt{u} \tag{21}$$

The product $R_0\alpha$ is equal to the slope of the curve of resistance plotted against air temperature and is approximately independent of the air temperature.

Two typical calibration runs are shown in table II and figure 7. In the table the details of the computation of the true speed u from the pressure developed by a reference static plate and the air density are omitted, since the procedure is well known. The two calibrations at the beginning and end of the series of observations show very satisfactory agreement. Such good agreement was not obtained in all cases, especially when the wire was subjected to speeds of 130 to 150 feet per second. In those instances where the calibration curves were different, an interpolation was made. In about one-third of the 62 series of observations made, the calibration curves at the beginning and end agreed as well as those shown in figure 7. In some 25 series the

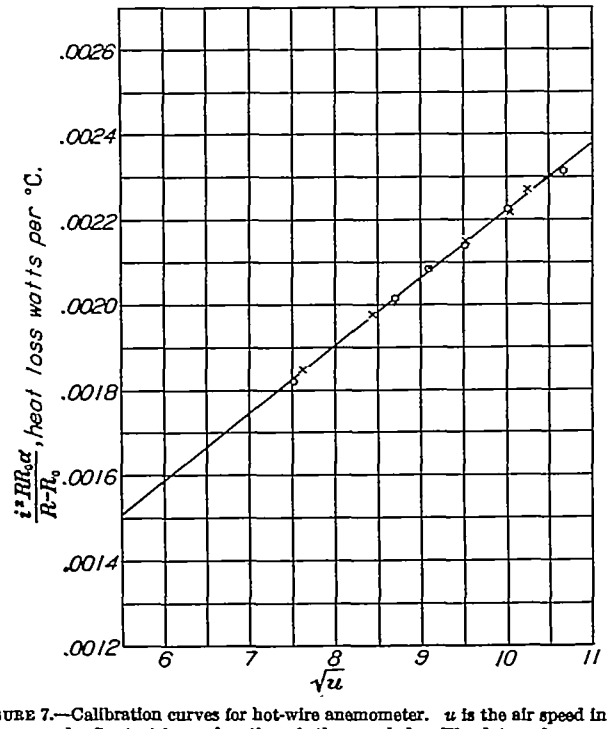

FIGURE 7.—Calibration curves for hot-wire anemometer. u is the air speed in feet per second. See text for explanation of other symbols. The dots and crosses distinguish the calibrations at the beginning and end of a series of observations of distribution of mean speed and speed fluctuation.

difference corresponded to a shift in the value of u/U_0 of 0.01 to 0.03, so that the interpolated values have a probable precision of about 0.01. In the remaining 16 series, the difference corresponded to a shift in u/U_0 greater than 0.03, rarely exceeding 0.06. In these cases the interpolated values have a probable precision of about 0.02. The use of the small diameter wire required to obtain fluctuation measurements impairs somewhat the precision of the measurements of mean speed.

Determination of the mean speed.—The determination of the mean speed in one series is illustrated in table III. The detailed micrometer readings and potentiometer readings are omitted, only the final values of y and of the voltage drop being given. The procedure may seem somewhat cumbersome, since one might plot the observed voltage drop in the calibration runs against speed and from such curves read off the speeds corresponding to the observed voltage drop in table III. The advantage of the procedure followed is the linear form of the calibration curve and its independence of air temperature. The final values obtained are not significantly affected by comparatively large changes in R_0 and α so that these quantities do not need to be known with high precision.

Heat loss due to presence of the plate.—When a hot-wire anemometer is used near a solid wall, the heat loss at a given speed is probably affected by the presence of the wall. In still air, the effect is quite perceptible at distances of about 0.08 inch from the wall. The magnitude of the effect is known to be a function of the speed, decreasing as the speed increases (reference 20). No entirely satisfactory procedure has been devised to correct for this effect.

Van der Hegge Zijnen determined the heat loss in still air as a function of the distance from the surface and the temperature difference between the wire and the surroundings. He then deducted from the observed heat loss in his experiments the excess heat loss found in still air at the same distance and temperature difference above the heat loss at a large distance from the plate.

A similar determination of the heat loss in still air was made in the present series of experiments and it was found that for temperature differences θ from 100° C. to 400° C., distances y 0.004 to 0.070 inch, the heat loss H_p due to the plate could be represented by the empirical formula

$$H_p=0.0000000127\frac{l}{y}\theta^2 \qquad (22)$$

where l is the length of the wire in inches, and H_p is measured in watts.

The result of applying this correction to the results of table III is shown in table IV. The value of u/U_0 at $y=0.015$ inch is reduced by 0.05.

Van der Hegge Zijnen noted that in some instances application of the correction gave S-shaped curves. He also found that the speed-distribution curves did not pass through the zero of the diagram and he arbitrarily decreased the y values by amounts from 0 to 0.005 inch to make them pass through zero. It is significant that application of the heat-loss correction based on still air determinations will produce a change in the intercept on the y axis in the direction observed.

On the basis of the results obtained for the laminar part of the boundary layer, which will be discussed later and the results of Schubauer (reference 21), it seems best to make no correction for heat loss when the flow is laminar and the speed is greater than 3 feet per second. In the absence of further information on the behavior of the wire when the flow is eddying, no correction has been made in that case either.

Determination of fluctuations.—The root-mean-square fluctuation in speed may be determined by measuring the root-mean-square fluctuation in voltage drop across the wire by means of a calibrated amplifier suitably compensated for the lag of the wire. Since the cooling is approximately independent of the direction of the air flow, the fluctuations are fluctuations of the absolute value of the velocity but, since the u-component of the fluctuation adds algebraically to the mean speed u whereas the v-component is at right angles, the fluctuation is primarily the u-fluctuation and is so designated in this paper.

The relation between speed fluctuation and voltage fluctuation may be found by differentiating (21) permitting i and R to vary, as follows:

$$\frac{2iRR_0\alpha}{R-R_0}di-\frac{i^2R_0^2\alpha}{(R-R_0)^2}dR=\frac{B}{2}\frac{du}{\sqrt{u}} \tag{23}$$

To connect di and dR, we have the relation

$$12=i(R+r) \tag{24}$$

where 12 is the battery voltage and r is the resistance of the heating circuit, excluding that of the wire. Hence

$$di=\frac{-idR}{R+r}=\frac{-i^2dR}{12} \tag{25}$$

and we find on substitution in (23), setting $i\,dR=dE$

$$\frac{du}{u}=-\frac{2}{B\sqrt{u}}\left[\frac{iR_0^2\alpha}{(R-R_0)^2}+\frac{1}{6}\frac{i^2RR_0\alpha}{R-R_0}\right]dE \tag{26}$$

If root-mean-square values are considered, the minus sign may be omitted.

A typical determination, omitting details of the computation of the compensation resistance and calibration of the amplifier, is shown in table V.

If a correction had been applied for heat loss according to (22), it is easily shown that a third term is added within the brackets on the right-hand side of (26) equal to $\frac{0.000\ 000\ 0127}{yiR_0\alpha}$. The effect of making this correction to the results of table V is shown in table VI. The values of $\frac{du}{u}$ are modified but there is very little change in the values of $\frac{du}{U_0}$.

Fairing of results for preparation of contour diagrams.—In order to prepare contour diagrams, the results of each series were plotted as shown in figure 8 and values read from faired curves at even intervals of u/U_0 and du/U_0 as illustrated in table VII. The x and y Reynolds Numbers were computed. It may be remarked in passing that figure 8 illustrates the distribution of mean speed and u-fluctuation near the beginning of the transition region.

It does not seem practicable to present the original observations of the 62 series of observations. The sample series gives some idea of the precision and accuracy of the observations. In general, it is believed that the errors in y do not exceed 0.003 inch (except in the preliminary series A), the errors in u/U_0 do not exceed 0.02, and the errors in $100\,\frac{du}{U_0}$ do not exceed 0.2 except for the very high values in the transition region. The contour diagrams used to present the results can be read easily to this precision.

No corrections have been applied for heat loss to the plate.

PRELIMINARY MEASUREMENTS WITH PRESSURE GRADIENT

The measurements now regarded as preliminary measurements (series A) were not so intended when the work was begun. They are here reported in spite of some inadequacies because some of the results are of interest and the experiments with pressure gradient were not repeated with the improved equipment.

The plate (fig. 5) and the traversing apparatus have already been described. The equipment was installed in the wind tunnel and the plate was alined to give a symmetrical wake as determined by a pitot tube. This installation required setting the plate at an angle of approximately 0.1° to the axis of the tunnel. Although

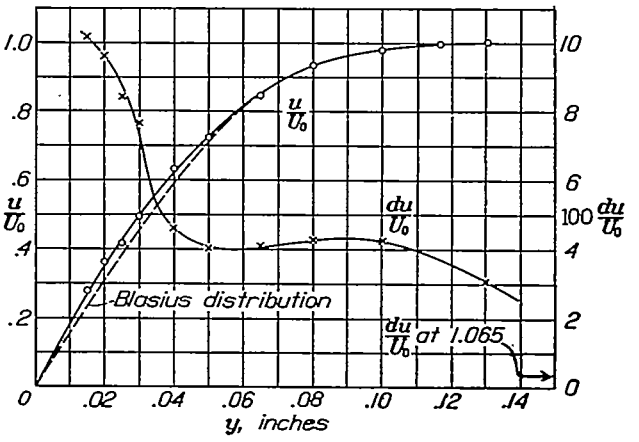

FIGURE 8.—Distribution of mean speed and u-fluctuation at x=23 inches for U_0=105.2 feet per second. Turbulence of free stream, 0.5 percent.

this necessity indicated at once that the leading-edge form was probably not the most desirable one, it was decided to proceed with some measurements.

The pressure gradient along a line parallel to and 9 inches from the plate is shown in figure 9. For the most part the pressure gradient is not constant. There is, however, a distance of about 2 feet, beginning about 8 inches downstream from the leading edge, over which the pressure falls at the rate of about 1.7 percent of the velocity pressure per foot.

The test speed chosen was approximately 100 feet per second. If transition had occurred at the same x-Reynolds Number (300,000) as in the measurements of van der Hegge Zijnen, it should have been found 6 inches behind the leading edge. Measurements at 6.32 inches and 17.5 inches gave distributions of mean speed of the laminar type although the u-fluctuations were considerably larger than in the general flow. After some study of a very pronounced disturbance

at the leading edge, measurements were made at 35.63 inches from the leading edge where the flow still was of the laminar type. The speed was then increased to 145 and finally to 175 feet per second, at which speeds the transition type of distribution was found at a distance of about 35 inches.

The results of the measurements of mean speed are shown in figure 10, omitting two runs which will be discussed separately. Transition begins at an x-Reynolds Number of approximately 1,800,000. From the plot the values of y appear to be subject to a systematic error, since the 0.3 speed contour is much closer to the wall than three times the distance between the 0.3 and 0.4 speed contour. A detailed study by means of cross plots and comparison with the Blasius distribution led to the conclusion that the values of y are probably too small by about 0.008 inch, corresponding at a speed of 102 feet per second to a displacement of the values of R_y by 400. It appeared

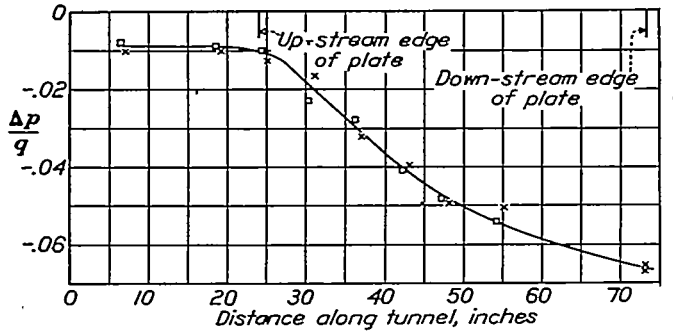

FIGURE 9.—Pressure gradient for measurements of series A (figs. 10 to 14, inclusive). q is the reference velocity pressure. The crosses denote measurements of static pressure; the circles, changes in the velocity pressure plotted with sign reversed. The velocity pressure increases as the static pressure decreases but at the same rate.

that the mounting of figure 5 was not sufficiently rigid. It was found that the mounting vibrated somewhat in the wind with a vibrating motion of perhaps 0.005 inch at the wire. For this reason no great reliance can be placed on the values of y, but the general character of the speed distribution and the value of the x-Reynolds Number for transition are not affected by this uncertainty.

Two runs which have been omitted from figure 10 are worthy of special consideration. After the observations at 102 feet per second were completed, observations were made at 145 feet per second, beginning at a distance of 35.3 inches from the leading edge, then 29.44 inches, each giving a transition type of curve. On the following day measurements were made at 23.31 inches and, surprisingly, the distribution was that characteristic of fully developed turbulent flow. This result seemed unreasonable and the next day a repeat run was made without disturbing the apparatus. The curve obtained was of the transition type, not checking the previous run. A week end intervened and 3 days later a second repeat run was begun. After one observation, which appeared to fall in with the immediately preceding run, it was noticed that the plate was somewhat dusty and it was decided to clean the plate. This was done and the run continued. The distribution then observed was of the laminar type, the run being that plotted in figure 10 for an x-Reynolds Number of 1,615,000.

The three distributions, all obtained within a few days under presumably identical conditions except for the amount of dust on the plate, are shown in figure 11. This plot gives the essential difference in character of the distribution of mean speed in the laminar, transition, and eddying regimes.

The corresponding u-fluctuations are shown in figure 12. There are illustrated the characteristic distributions of u-fluctuations for the laminar, transition, and eddying regimes.

The observations of u-fluctuations are hardly complete enough to enable the plotting of an accurate contour diagram. The values from faired curves are indicated in figure 13, the two runs previously discussed being omitted. The solid contours are drawn on the assumption that the observations at x-Reynolds Numbers of 117,000 and 1,773,000 are not to be considered. Since the necessity of keeping dust removed from the plate was not appreciated, the various measurements may not be comparable. The location of the contours has been guided to some extent by the results of the later measurements.

One interesting feature is the disturbance near the leading edge. The u-fluctuation in the free stream was only 0.5 percent of the mean speed, whereas in this disturbance the u-fluctuation is 5.0 percent of the mean speed in the free air stream. Evidently the stagnation point is on the inclined leading edge and the flow around the sharp corner sets up an increased turbulence. This turbulence is damped out to some extent along the plate, then increases, slowly at first, but very rapidly in the transition region. The primary purpose of presenting these exploratory measurements is to show that with an accelerating pressure gradient present the strong leading-edge disturbance is not sufficient to produce an early transition.

At 35.5 inches, the flow was still of the transition type, so that completely eddying flow was not obtained in this series of measurements.

When it was realized that the traverse mechanism was not giving sufficiently accurate values of y, that the leading edge shape was very poor, that the plate must be kept free of dust, and that the influence of the pressure gradient was very large, it was decided to make a completely fresh start.

MEASUREMENTS WITH SMALLER PRESSURE GRADIENT

Normal air stream.—As already described a new plate was obtained with sharp symmetrical leading edge and a new traversing mechanism was constructed (fig. 6). In addition, an attempt was made to secure the condition of zero pressure gradient. It was first thought that the desired result might be obtained by a

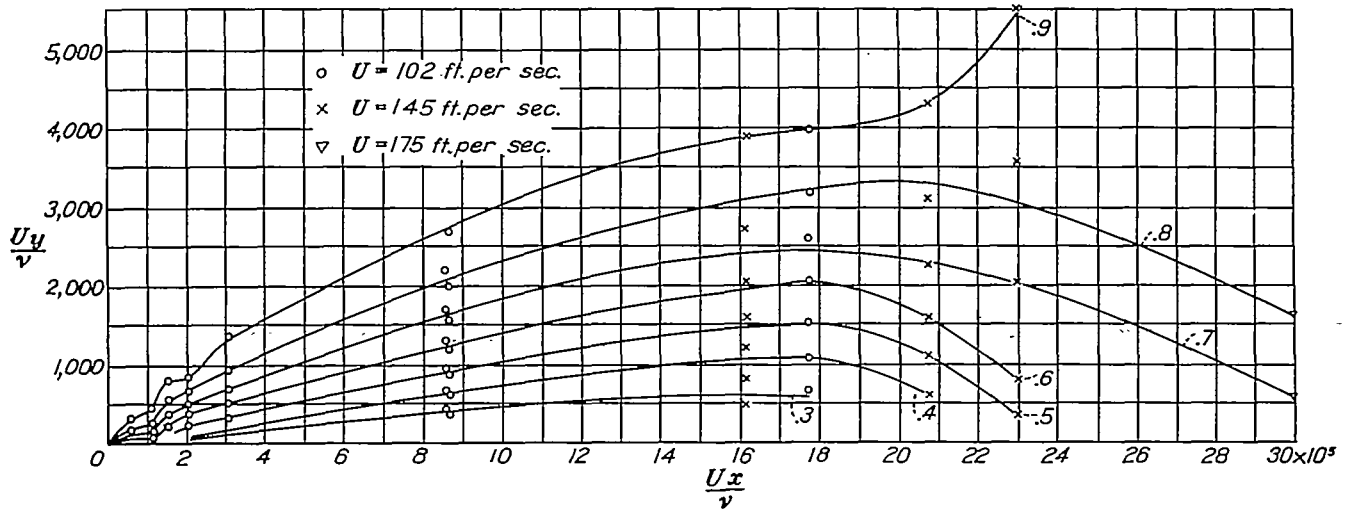

FIGURE 10.—Distribution of mean speed, preliminary series A, with pressure gradient of figure 9, turbulence of free stream, 0.5 percent. See legend of figure 1 for notation. U, the speed of the free stream, increases slightly along the plate. The contours are contours of equal u/U.

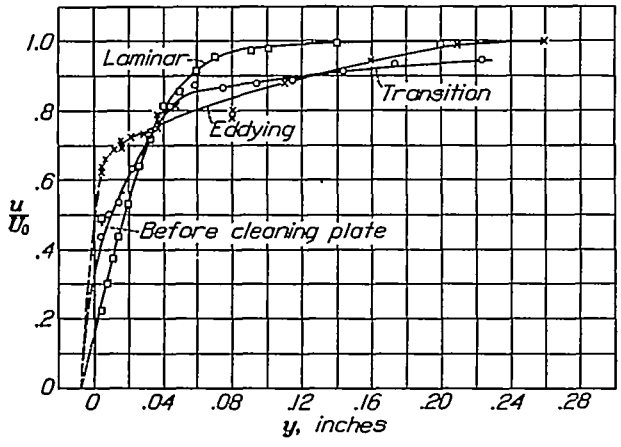

FIGURE 11.—Distribution of mean speed at $x=23.3$ inches for $U=145.2$ feet per second, showing effect of roughness produced by dust on the plate. The three curves illustrate distributions of the laminar, transition, and eddying types.

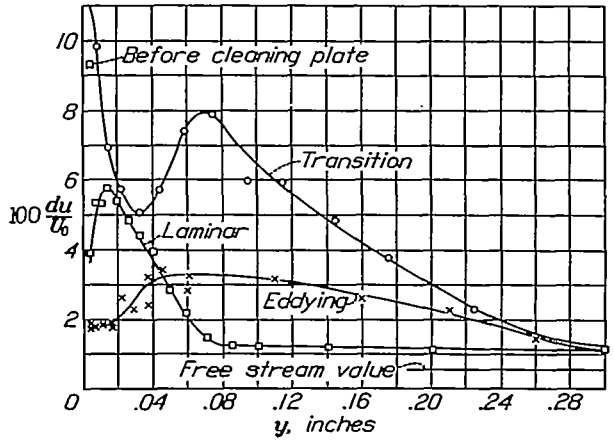

FIGURE 12.—Distribution of u-fluctuation at $x=23.3$ inches for $U=145.2$ feet per second, showing effect of roughness produced by dust on the plate. The three curves illustrate distributions of the laminar, transition, and eddying type.

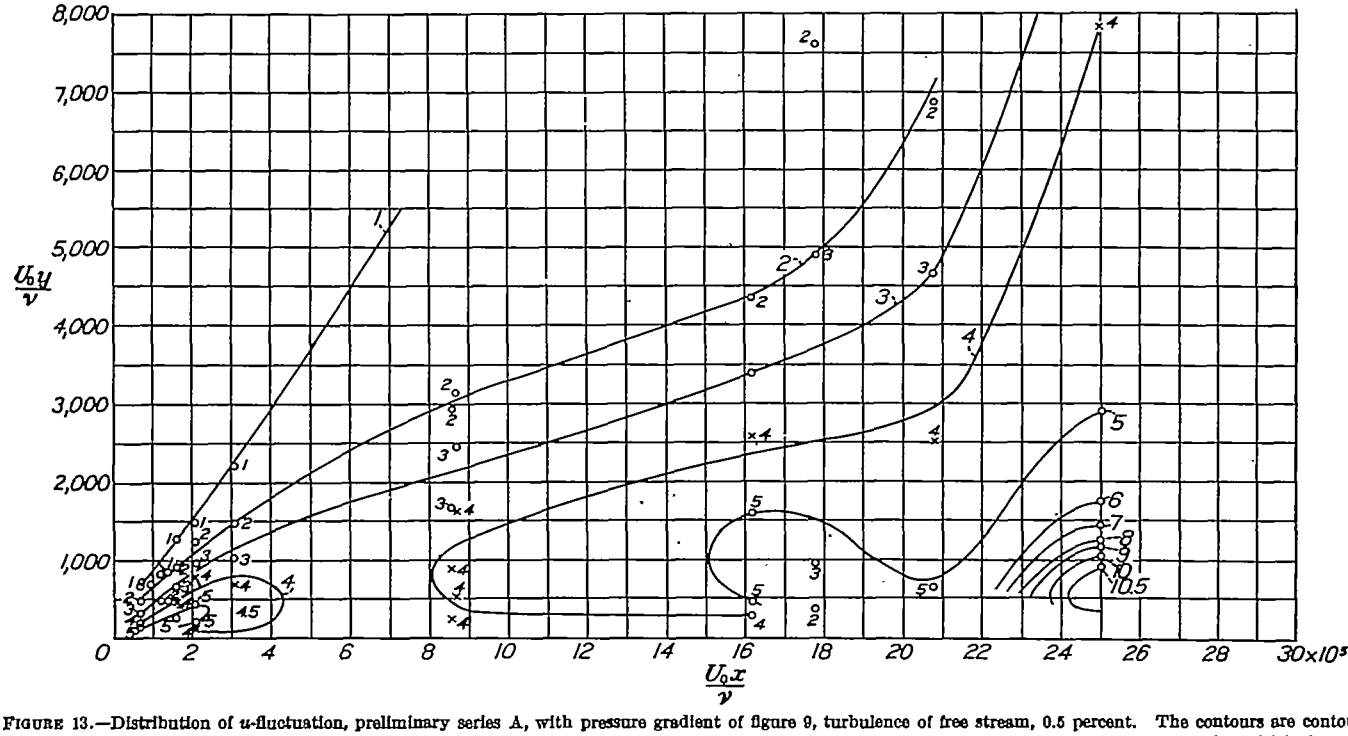

FIGURE 13.—Distribution of u-fluctuation, preliminary series A, with pressure gradient of figure 9, turbulence of free stream, 0.5 percent. The contours are contour of equal values of the root-mean-square speed fluctuation expressed in percent of the speed of the free stream. See legend of figure 1 for notation. Note intense leading edge disturbance.

136692—37——24

slight inclination of the plate to produce an expanding cross section between the working side of the plate and the wall. Pressure surveys showed considerable local variations near the plate of the nature found for small

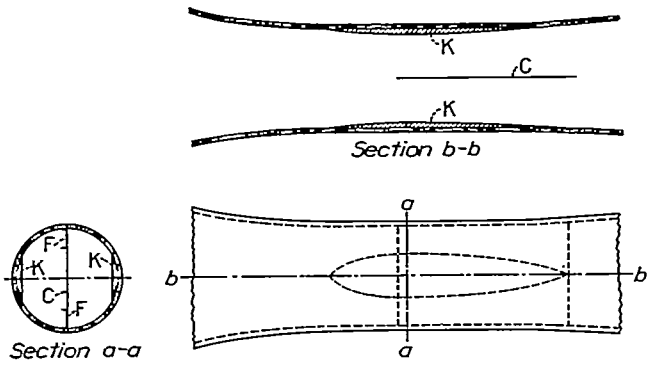

FIGURE 14.—"Blisters" installed in wind tunnel to reduce pressure gradient.

Several weeks were spent in modifications of the contour of the blisters to secure approximately zero pressure gradient. The ideal was in no wise attained and the first series of measurements with the improved

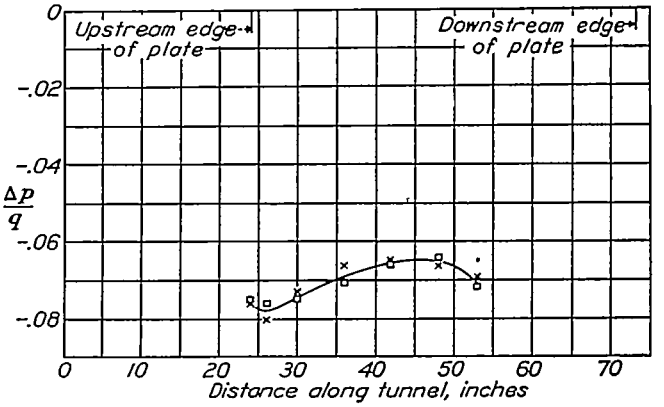

FIGURE 15.—Pressure gradient for measurements of series B and D (figs. 16 to 22, inclusive). See legend of figure 9. The speed of the free stream departs from the mean value by a maximum of 0.4 percent.

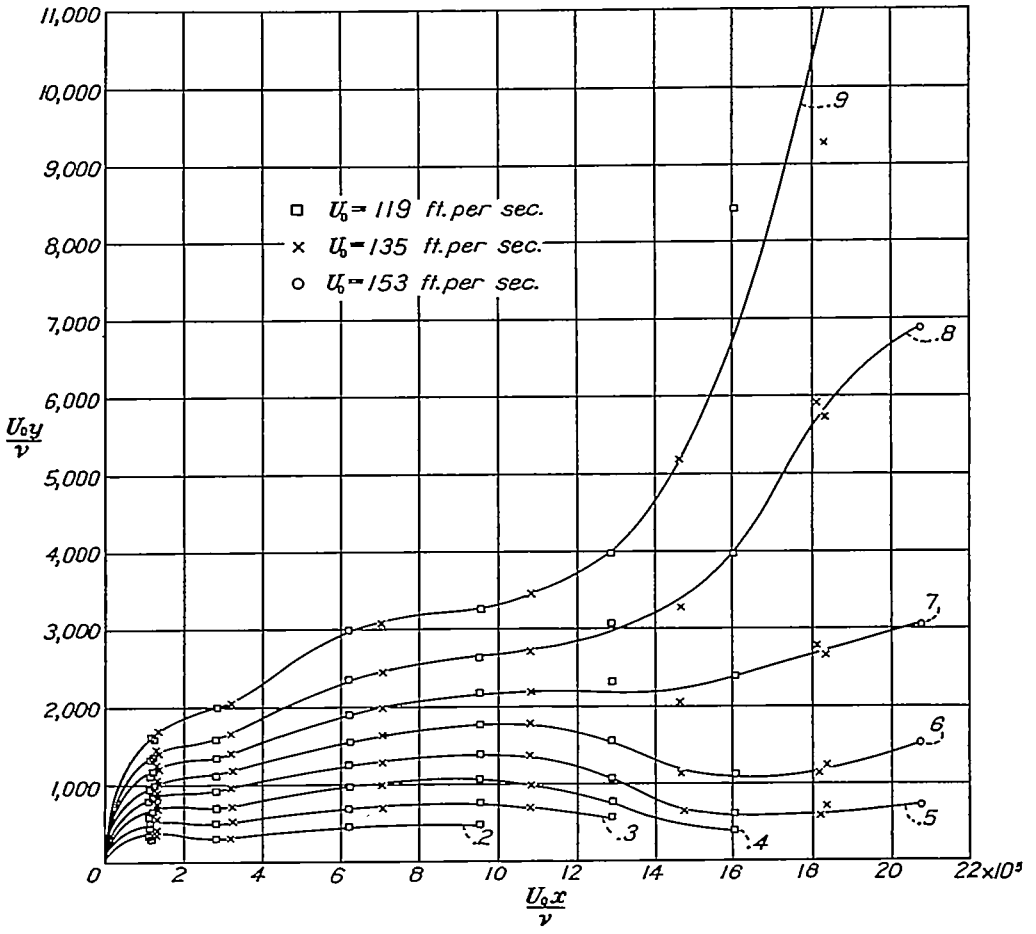

FIGURE 16.—Distribution of mean speed, series B, with pressure gradient of figure 15, turbulence of free stream, 0.5 percent. See legend of figure 1 for notation.

plates set at a small angle of attack. Attention was then turned toward producing the expanding cross section by suitable blocking at the tunnel walls. The general form and scale of the "blisters" applied to the tunnel wall is shown in figure 14 at K.

apparatus was made under the pressure gradient shown in figure 15. The pressure falls slightly for 2 inches, then rises at the rate of about 0.9 percent of the velocity pressure per foot for about 19 inches, then falls at a rate of about 1 percent of the velocity pressure per

foot. By comparison with figure 9, the total range in pressure has been reduced to one-fourth of that previously found and the maximum gradient has been reduced to about one-half that previously found, with gradients of both signs occurring.

In the first series of measurements (series B), only mean speeds were determined. Sixteen traverses were

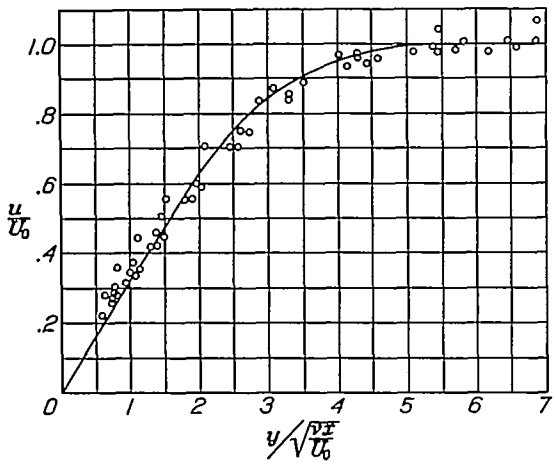

FIGURE 17.—Distribution of mean speed, for x=5, 11, and 17 inches, series B, plotted for comparison with the Blasius distribution.

made in all, at distances 2, 5, 11, 17, 22.8, and 28.8 inches from the leading edge, at speeds of 119 and 135 feet per second except for one run at 28.8 inches for which the speed was 153 feet per second. The contour

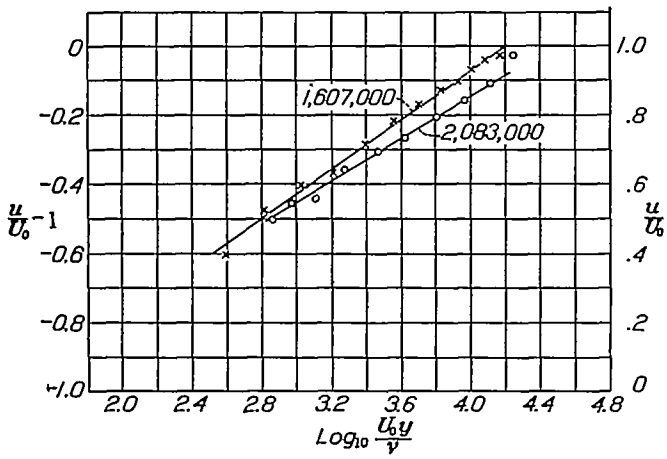

FIGURE 18.—Distribution of mean speed, for x-Reynolds Numbers 1,607,000 and 2,083,000, series B, plotted for comparison with the logarithmic distribution.

diagram prepared from faired curves similar to figure 8 is shown in figure 16.

Transition begins at an x-Reynolds Number of about 1,100,000. The observations for the several speeds are quite concordant and there is no indication of any systematic error in the values of y, except possibly at the 2-inch station (x-Reynolds Number about 120,000).

Figure 17 shows that the results for the 5-, 11-, and 17-inch stations are in very satisfactory agreement with the Blasius theoretical curve. In this figure, the original observations, not faired values, are plotted. The agreement would not have been so good had the heat loss to the wall in still air been applied as a correction to the observed heat loss.

The data available in the eddying region are hardly sufficient to make possible any extensive analysis. In figure 18 observations for x-Reynolds Numbers of 1,607,000 and 2,083,000 are plotted in a form suggested by equation (15). This equation represents the data

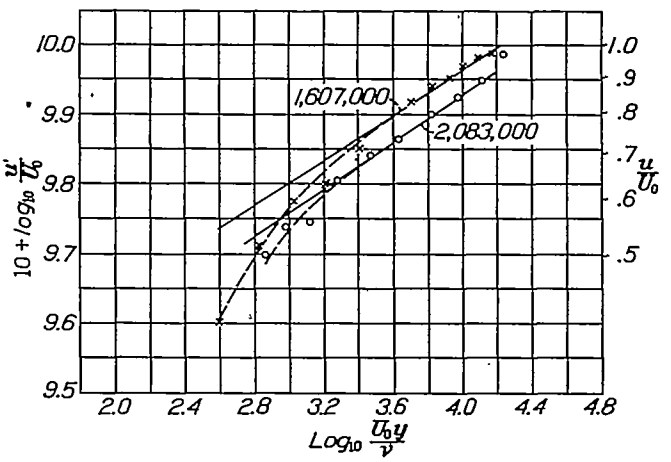

FIGURE 19.—Distribution of mean speed, for x-Reynolds Number 1,607,000 and 2,083,000, series B, plotted for comparison with the power-law distribution.

well within the precision of the observations over a wider range than the power law representation shown in figure 19. The lines drawn in figure 19 correspond to exponents of 0.16 and 0.17.

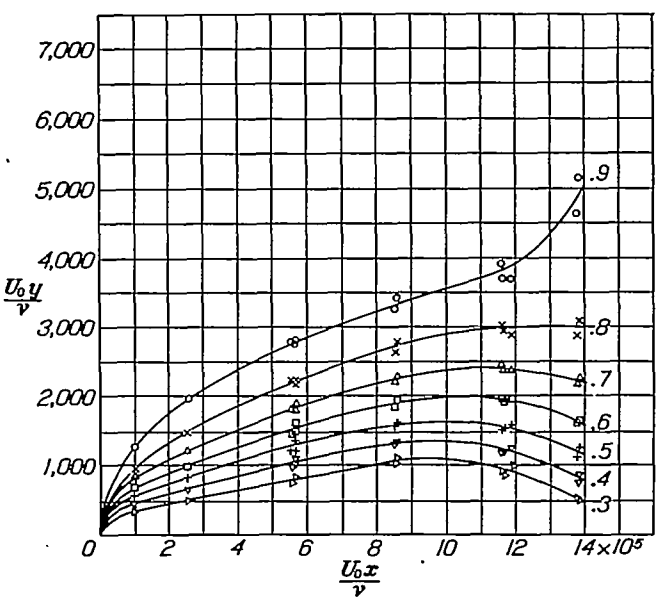

FIGURE 20.—Distribution of mean speed, series D, with pressure gradient of figure 15, turbulence of free stream, 0.5 percent. See legend of figure 1 for notation.

The first series of measurements of mean speed only (series B) was made during the month of June 1930. In October, after the completion of some measurements with increased turbulence of the wind stream, a second series of measurements (series D) was made in which both mean speed and u-fluctuations were determined. Twelve traverses were made, at distances of 2, 5, 11, 17, 23 and 28 inches, at a speed of 105

feet per second. The contour diagram of the distribution of mean speed is shown in figure 20.

Comparison of the original observations for the 2-, 5-, 11-, and 17-inch stations with the Blasius curve is made in figure 21. There is some evidence of a systematic error in y of the order of 0.001 inch, the observed values being too large. From the construction of the traverse mechanism, the effect of wind load on the prongs would be to deflect the mounting toward the plate. Such an effect is not indicated, however, in the earlier series (fig. 17). In view of the difficulty of the measurements, it seems quite clear that the Blasius curve is an accurate representation of the laminar portion of the velocity field near a plate with sharp

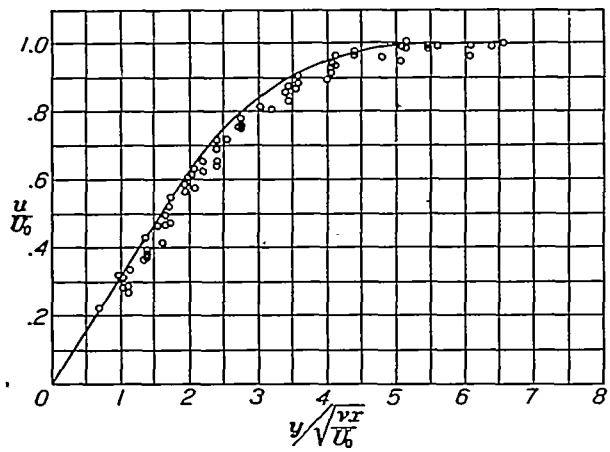

FIGURE 21.—Distribution of mean speed, for x=2, 5, 11, and 17 inches, series D, plotted for comparison with the Blasius distribution.

symmetrical leading edge in a stream without appreciable pressure gradient.

No observations of this series fall within the eddying region.

The contour diagram of the u-fluctuations is shown in figure 22. It is not possible without greatly confusing the diagram to show either original observations or faired values. In one traverse at 11 inches, the fluctuations were abnormally large and not concordant with two additional traverses at the same station. The cause is not known, and results for this one traverse have not been considered. Otherwise, the individual traverses were reasonably concordant, and it has only been necessary to smooth out minor inconsistencies. The faired values from which figure 22 was prepared are given in table VIII. The u-fluctuation in the free air stream was 0.5 percent of the mean speed.

The interesting features of figure 22 are the leading-edge disturbance, which has not been completely eliminated; the fluctuations in the laminar region of magnitude about three times the free-stream fluctuation; the increasing amplitude of fluctuation beginning at an x-Reynolds Number of 700,000, as compared, with transition at 1,100,000 as inferred from the distribution of mean speed; and the large amplitude of fluctuation in the transition region.

Artificially turbulent air stream.—The very high value of the x-Reynolds Number, 1,100,000, for transition, as compared to the value 300,000 observed by van der Hegge Zijnen and Hansen, is undoubtedly to be attributed to the small magnitude of the u-fluctuations in the normal air stream of the 3-foot wind tunnel. In order to definitely confirm this statement, the turbulence was artificially increased by the introduction of a wire screen of ½-inch mesh 39 inches ahead of the leading edge of the plate. Some 200 small aluminum tags about 1¼ inches by 1 inch by 1/32 inch were fastened to the screen by paper clips. The tags, fluttering in the wind, produced a large distributed u-fluctuation whose root-mean-square value was about 3.0 percent of the mean speed of the air stream. The fluctuations normally present were accordingly increased by a factor of 6.

The u-fluctuation decreased slightly along the plate, from about 3.2 percent at the leading edge to about

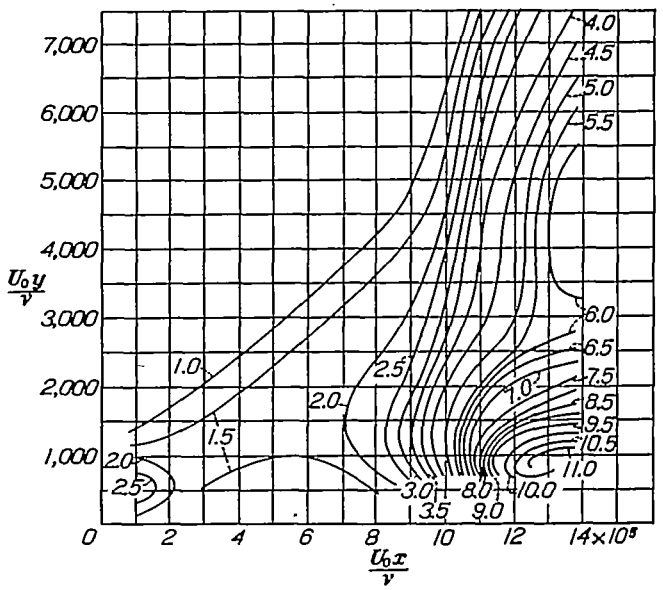

FIGURE 22.—Distribution of u-fluctuation, series D, with pressure gradient of figure 15, turbulence of free stream, 0.5 percent. See legend of figure 13.

2.8 percent at 28 inches from the leading edge. The maximum single value observed was 3.42 and the minimum, 2.56 percent.

The pressure gradient along the plate was that shown in figure 23. The variation is similar to that of figure 15, but the approximation to constant pressure was somewhat better.

Twelve traverses were made at a speed of about 65 feet per second at distances 2, 4, 5, 6, 7, 8, 10, 11.5, 13, 18, 23, and 28.5 inches from the leading edge, and ten traverses were made at a speed of about 32.5 feet per second at distances 4, 8, 10, 12, 14, 16, and 28 inches. In six cases, therefore, approximately the same x-Reynolds Number was obtained at two speeds differing by a factor of 2. The choice of speeds considerably lower than 100 feet per second permitted some increase in precision. The contour diagram prepared from faired curves is shown in figure 24.

Transition begins at an x-Reynolds Number of the order of 100,000; i. e., very close to the leading edge. The results for the two speeds are reasonably concordant and, in the six cases where the same Reynolds Number was obtained at the two speeds, there is no

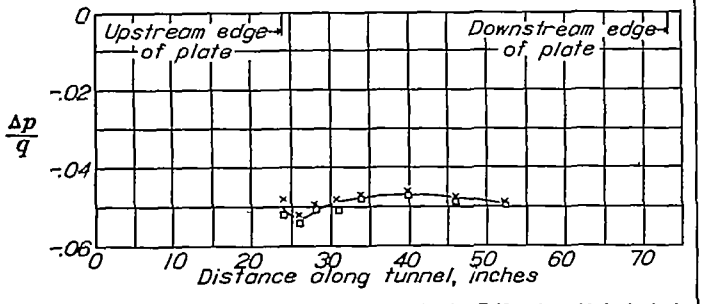

FIGURE 23.—Pressure gradient for measurements of series C (figs. 24 to 26, inclusive). See legend of figure 9. The speed of the free stream departs from the mean value by a maximum of 0.2 percent.

evidence of a systematic difference. Comparison of figure 24 with figures 16 and 20 will emphasize the very great influence of the initial turbulence of the wind tunnel on the velocity distribution and hence on the skin friction. Only the measurements at the

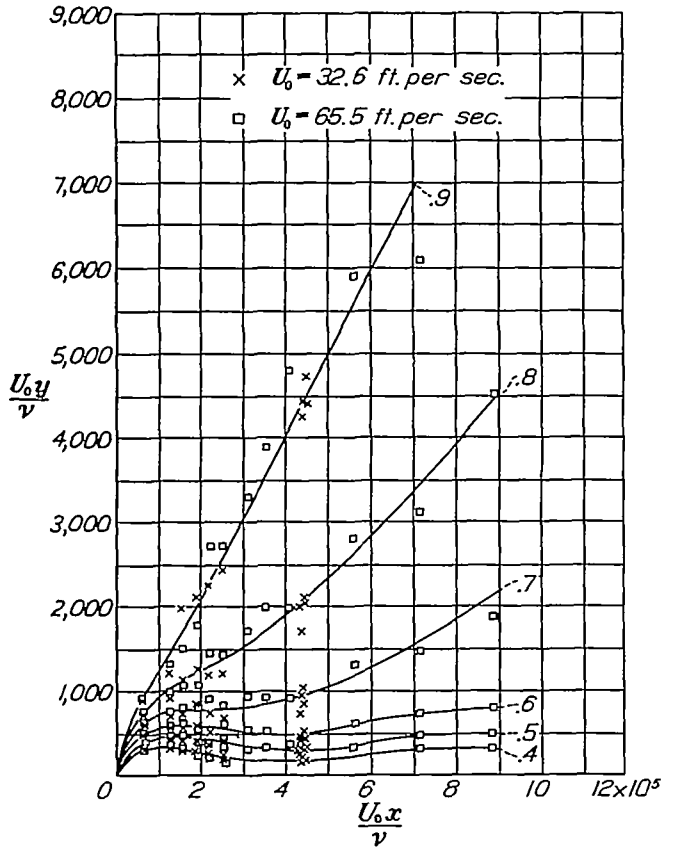

FIGURE 24.—Distribution of mean speed, series C, with pressure gradient of figure 23, turbulence of free stream, 3.0 percent. See legend of figure 1 for notation.

2-inch station are in the laminar region. These two traverses agree well with the Blasius distribution.

Figure 25 shows the results of four traverses in the eddying region at an x-Reynolds Number of approximately 435,000 and one traverse at 888,000 plotted in the form suggested by equation (15). The four repeat runs show that the precision of the measurements is not sufficiently great to determine the slope with very great accuracy.

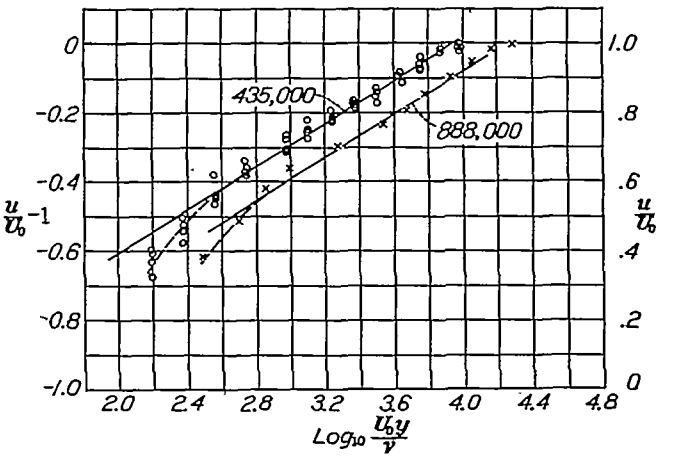

FIGURE 25.—Distribution of mean speed, for x-Reynolds Numbers 435,000 and 888,000, series C, plotted for comparison with the logarithmic distribution.

The contour diagram of the u-fluctuation is shown in figure 26. The faired values from which the dia-

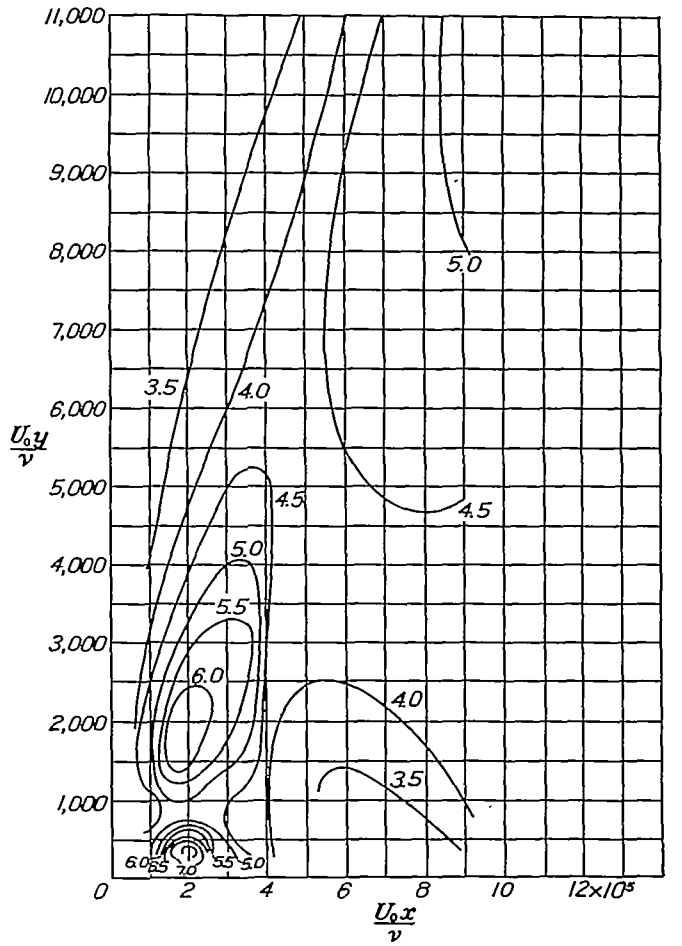

FIGURE 26.—Distribution of u-fluctuation, series C, with pressure gradient of figure 23, turbulence of free stream, 3.0 percent. See legend of figure 13.

gram was prepared are given in table IX. The region of maximum u-fluctuation occurs at an x-Reynolds Number of about 200,000, corresponding roughly to the middle of the transition region. In the eddying

region the magnitude of the fluctuation is of the order of 4 or 5 percent of the mean speed as compared with the free stream value of about 3 percent.

DISCUSSION

Meaning of fluctuations in laminar region.—The distinction between laminar and eddying flow is usually based on the nature of the variation of the skin friction with speed or on the nature of the speed distribution as has been more fully discussed in the section on Previous Experimental Work. The skin friction and speed distribution in laminar flow are generally computed on the assumption of steady flow, and the agreement between experimental results and theoretical calculations leads us to picture the laminar flow near a plate as a steady flow. The experiments described in this paper clearly show that the conclusion is incorrect; the experiments together with the computations illustrated in figures 3 and 4 indicate that it is possible to have large speed fluctuations with no measurable effect on the distribution of mean speed.

On the other hand, it has long been known that eddying flow is characterized by fluctuations of speed at a given point and hence there is a temptation to identify speed fluctuations with turbulence. Here again the experiments described in this paper show that large fluctuations are not confined to the region of eddying flow. It is not possible to determine by measurement of amplitude of fluctuation alone whether the flow is laminar or eddying.

This result and a brief account of the measurements described in this paper were reported to the Fourth International Congress of Applied Mechanics at Cambridge, England, in 1934. Tollmien discussed this account in reference 22 and emphasized by examples the importance of considering the correlation between the several components of the velocity fluctuations. He says "In order to produce a shearing stress a correlation is necessary between the components of the velocity fluctuations in two different directions. This is of course well known. But one has hitherto frequently regarded the mere existence of velocity fluctuations as sufficiently characteristic of turbulence in the tacit expectation that a correlation between the components of the fluctuations would be present. It is therefore necessary in general to give the greatest attention to the correlation between any, even theoretical, velocity fluctuations which have been determined, in order to be certain of the effect of the fluctuations on the form of the velocity distribution curve." One of the interesting examples in Tollmien's paper is the von Kármán vortex street, which shows no correlation between the longitudinal and lateral components of the velocity fluctuations.

It may be remarked that the fluctuations in the free stream of the wind tunnel are of this uncorrelated type having no influence on the distribution of mean speed. Since these fluctuations have generally been called "turbulence", the author denotes a flow with the correlated type of fluctuations as "eddying" flow. Whether these particular names are generally adopted or not, there should be some clear distinction by means of different names between fluctuations whose components are uncorrelated and those which show correlation. Most experimenters would consider the flow in a von Kármán vortex street as highly turbulent.

In the discussion at the Congress of Applied Mechanics, it was pointed out that the fluctuations in the laminar layer were, generally speaking, of lower frequency than the fluctuations in the eddying layer. At the time the measurements described in this paper were made, a suitable oscillograph was not available. In 1934, after the Cambridge meeting, a plate was installed in the 4½-foot wind tunnel at the National Bureau of Standards and records of the fluctuations made with a cathode ray oscillograph. For convenience, the flow was made more turbulent by a wire screen of 1-inch mesh placed about 4.5 feet upstream from the plate. The u-fluctuation of the free stream was approximately 1.3 percent of the mean speed, giving transition at an x-Reynolds Number of about 500,000. The pressure gradient was not determined and the values of y were not accurately measured; hence these values are not comparable with the data reported in the preceding section. The records obtained are shown, in part, in figure 27. They were not made simultaneously. It is seen that the fluctuations in the laminar region (position 2) are much less rapid than those in the eddying region (position 5).

It should perhaps be pointed out that "slow" and "fast" are in this connection purely relative terms, the absolute magnitude of the rate of change of speed being a function of mean speed and of the thickness of the boundary layer. In any given flow, the distinction between laminar and eddying flow can be made on this basis, but in two different flows at widely different speeds and with boundary layers of widely different thickness, the use of this simple criterion would not be safe.

In the opinion of the author, the fluctuations in the laminar layer are to be regarded as forced oscillations produced by the turbulence of the wind-tunnel air stream. The qualitative distribution is very similar to that computed in the highly simplified manner described in the theoretical treatment of the transition and pictured in figure 4. Since, however, the distribution in the "free" oscillations as computed by Schlichting (reference 23) is also of much the same character, the general shape of the distribution curve cannot serve as a criterion of whether the fluctuations are forced or free.

Transition from laminar to eddying flow.—Figures 1, 10, 16, 20, and 24 show a gradual transition region extending over a range of x-Reynolds Numbers of 200,000 or more. It is very difficult to state definitely where the transition begins. The departures from the

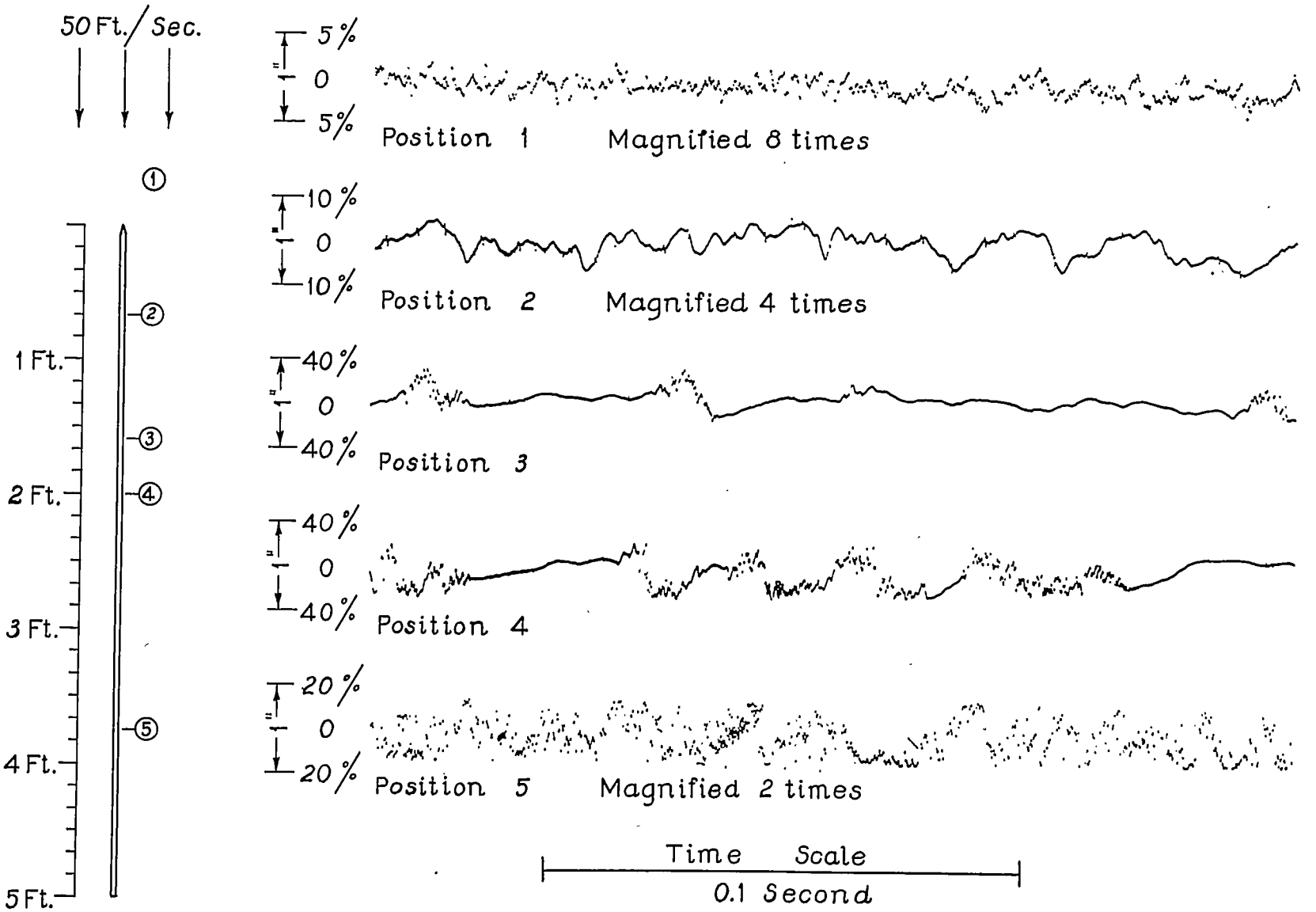

FIGURE 27.—Oscillograph records of u-fluctuation at several points near a plate.

Blasius distribution begin earlier for speed contours in the neighborhood of 0.4 or 0.5 than for the 0.9 contour. The layer begins to thicken rapidly at a somewhat greater x-Reynolds Number than that at which the speed near the surface begins to be accelerated. The character of the first noticeable change may perhaps best be seen in figure 8.

Figures 22 and 26 show that the rate of increase of the amplitude of the u-fluctuation is accelerated at an x-Reynolds Number considerably lower than that for which noticeable departures from the Blasius distribution of mean speed occur.

Finally, figure 27 shows that the transition is in fact a sudden phenomenon. Near the upstream limit of the transition region, eddying flow occurs intermittently at infrequent intervals, the flow being of the eddying type for only a small fraction of the time

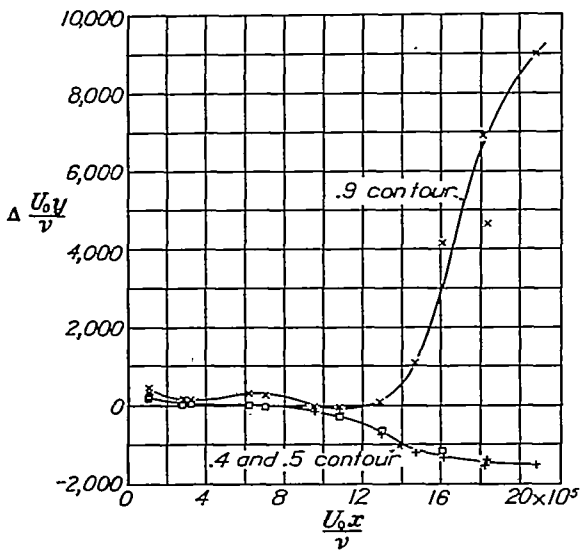

FIGURE 28.—Departure of the 0.4, 0.5, and 0.9 contours of mean speed in figure 16 from the Blasius positions. The ordinates represent the observed y-Reynolds Numbers for the speed contours minus the y-Reynolds Number computed from Blasius' solution for a laminar boundary layer.

covered by the record. Near the downstream limit, laminar flow occurs infrequently.

The process may be pictured somewhat as follows: Transition is a sudden phenomenon controlled by the instantaneous pressure distribution arising from the turbulence of the free air stream. As the pressure distribution fluctuates, the point of transition fluctuates back and forth along the plate. At a given point in the transition region the flow is sometimes laminar and sometimes eddying—more frequently laminar as the point of observation is moved upstream and more frequently eddying as the point is moved downstream. Since the turbulence of the free stream is constant only in a statistical sense, there is a point of transition only in a statistical sense. The designation of the Reynolds Number at which transition occurs becomes then a matter of definition.

No entirely satisfactory definition has been found. The values quoted can be regarded only as approximate. In figure 28, the departures of the distribution of mean speed of figure 16 from the Blasius distribution are plotted for the 0.4, 0.5, and 0.9 contours. The value of the x-Reynolds Number for transition has been given as 1,100,000. It is obvious that significant departures occur at a somewhat lower x-Reynolds Number for the 0.4 and 0.5 contours, perhaps as low as 900,000 whereas the 0.9 contour does not show significant departures until 1,300,000.

The use of a Reynolds Number based on the "displacement thickness" δ^*, which equals $\int_0^\infty (1-u/U_0)dy$, has often been suggested. A plot of δ^*-Reynolds Number against x-Reynolds Number, compared with a similar plot of the δ^*-Reynolds Number computed from the Blasius distribution, is not found to give clear indications of transition, because the departures

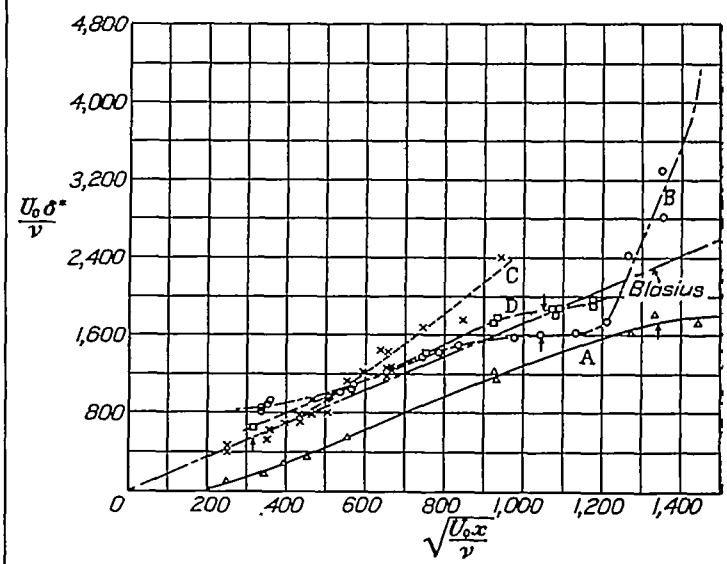

FIGURE 29.—The δ^*-Reynolds Number for the several series of observations as a function of the square root of the x-Reynolds Number. The transition begins at the values indicated by the arrows as determined from the distribution of mean speed.

from the Blasius distribution expressed as differences in y-Reynolds Number for a given speed are in one direction for the 0.4 and 0.5 contours and in the opposite direction for the 0.8 and 0.9 contours. The two effects partly compensate and lead to only moderate departures of the δ^*-Reynolds Number from the Blasius result, which are sometimes masked by experimental errors.

The comparison was made, however, and the results are given in figure 29. The values of the δ^*-Reynolds Number were computed by Simpson's rule from the faired values similar to those of table VII. Between the lowest value of u/U_0 (0.3 in table VII) and zero, a linear interpolation was used. The transition points are indicated in figure 29 by arrows. The points for the preliminary observations of series A show the apparent systematic error of about 400 in the value of $U_0 y/\nu$ to which reference has previously been made.

If correction is made for this shift, the δ^*-Reynolds Number at transition appears to be about 2,200.

Series B shows a somewhat earlier transition than series D as may also be seen from a careful examination of figure 16 and figure 20. In view of the difficulties of measurement, the results may be averaged to give a δ^*-Reynolds Number of about 1,700.

The curves for series A, B, and D show a bending away from the Blasius curve toward lower values with approach to slowly changing δ^*-Reynolds Number with increasing x-Reynolds Number. This deflection is followed for series B by a rapid increase. The same effects are not marked for the series C observations. From figure 24, it is clear that transition begins at an x-Reynolds Number of about 100,000 corresponding to a δ^*-Reynolds Number of about 560. No perceptible departure of the δ^*-Reynolds Number curve in figure 29 from the Blasius curve occurs until much higher values.

It is possible to suggest an unambiguous definition of the Reynolds Number of transition; for example, that for which the 0.4 contour deviates from the theoretical Blasius position by a y-Reynolds Number of 100. But so long as the effects of experimental errors combined with the effects of unavoidable departures from the uniform pressure assumed in the theory are of the order of 300 or 400, accurate determinations cannot be made in accordance with such a definition.

Effect of turbulence.—In the experiments of van der Hegge Zijnen and of Hansen, the turbulence of the air stream was not measured, no method then being known. From the dimensions of the honeycombs and their location and published data (for example, that in reference 17), we may estimate that the turbulence was between 1 and 2 percent. The corresponding x-Reynolds Number for transition was about 300,000, and the δ^*-Reynolds Number for transition about 940.

The experiments described in this paper give the following results:

Turbulence percent	x-Reynolds Number	δ^*-Reynolds Number
0.5	1,100,000	1,700
3.0	100,000	560

The available data do not suffice to construct a well-defined curve such as that established for the relation between the critical Reynolds Number of a sphere and the turbulence (reference 18). Nevertheless, there is little doubt that such a relation exists. The effect of turbulence is obviously very great. It is believed that the evidence presented supports the view that in an air stream of approximately uniform static pressure and for a smooth plate with sharp leading edge, the x-Reynolds Number for transition is a function of the turbulence varying from about 1,100,000 to 100,000.

Effect of pressure gradient.—The preliminary series of experiments showed that the effect of a pressure gradient such as shown in figure 9 was to increase the x-Reynolds Number for transition in a stream of turbulence 0.5 percent from 1,100,000 to 1,800,000. The change in the δ^*-Reynolds Number is not so definitely established in view of the apparent systematic error in the preliminary series, but the author believes that with the pressure gradient the δ^*-Reynolds Number was increased from 1,700 to about 2,200; in other words, approximately in the same ratio as the square roots of the x-Reynolds Numbers.

The effect of an accelerating pressure gradient is then to delay the transition. This effect does not contradict the picture of the mechanism of transition described in the theoretical treatment, for the addition of a steady accelerating pressure gradient to the fluctuating pressure gradients of the turbulence of the air stream would reduce the magnitude of the instantaneous retarding gradients and hence delay separation. It is interesting to speculate on the effect of an accelerating gradient so large as to suppress entirely the retarding gradients in the fluctuations. A fundamental investigation of the effect of pressure gradient with constant turbulence is urgently needed. It is desirable that such experiments be made with both low and high degree of turbulence in the air stream.

Speed distribution in eddying region.—From the slopes of the lines in figure 18 and von Kármán's value, 0.4, of the universal constant k, the local friction coefficient may be computed according to equation (15). The values obtained are 0.0076 and 0.0057, respectively, which are unreasonably high.

Similarly the slopes of the lines in figure 25 give values of the local skin-friction coefficient computed from equation (15) for $k=0.4$ of 0.0057 and 0.0062 which again are unreasonably high. From von Kármán's table (reference 16) values of the order of 0.0045 and 0.0038 would be expected. Such a large difference is not accounted for by any reasonable assumption as to the errors in the velocity determinations. Application of the still-air heat-loss correction would increase the discrepancy.

The explanation of the discrepancy is that in the thin boundary layer nearly all stations are sufficiently near the wall that the effects of viscosity cannot be neglected, the y-Reynolds Numbers being less than 4,000.

Since no independent determination of local skin-friction coefficients was possible in the present experiments, no direct comparison can be made. It is of interest, however, to estimate the local skin-friction coefficients c_f from von Kármán's table and to plot the distributions of figures 18 and 25 with $\left(\frac{2}{c_f}\right)^{1/2}\frac{u}{U_0}$ as ordinate and $\log_{10}\left(\frac{c_f}{2}\right)^{1/2}\frac{u}{U_0}$ as abscissa. This has been done in figure 30. The solid curve is that determined by von Kármán from Nikuradse's measurements in pipes. In the estimation of c_f, the Reynolds Number used was

that obtained by assuming the eddying layer to begin at the beginning of the transition region.

The measurements with artificial turbulence lie about 4 percent above von Kármán's curve but sensibly parallel. On the other hand, the measurements with very small turbulence in the air stream show a different slope. The exact significance of this difference is not clear. The speed fluctuation at the center of a pipe in which the flow is eddying is of the order of that at the outer edge of the boundary layer in the experiments with artificial turbulence. The observations now

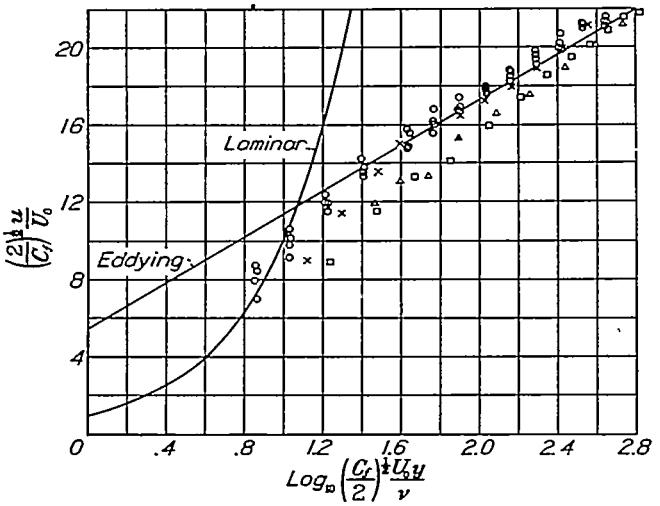

FIGURE 30.—Distribution of mean speed in eddying region for comparison with Kármán's formula. The data are those shown in figures 18 and 25. The local friction coefficient C_f, is estimated by assuming that the eddying begins at the beginning of the transition region.

available are too few to be certain that the shape of the speed-distribution curve near a plate is actually a function of the turbulence of the stream, as suggested by figure 30.

CONCLUSION

The intensive study of the boundary-layer flow near a thin flat plate promises to yield considerable information as to the origin of eddying flow and the effect of turbulence in wind-tunnel experiments. The information now available shows that the velocity field varies greatly with the turbulence of the air stream, and with the pressure gradient. The Reynolds Number at which transition occurs in a stream without pressure gradient decreases greatly as the turbulence is increased.

The presence of fluctuations is not an indication of the presence of eddy shearing stresses. The laminar layer shows speed fluctuations of amplitude considerably greater than that in the free stream. These fluctuations do not produce departures from the theoretical Blasius distribution for laminar flow. They are of lower frequency than the fluctuations in the eddying boundary layer.

Transition is a sudden phenomenon, but the point of transition moves back and forth within rather wide limits.

NATIONAL BUREAU OF STANDARDS,
WASHINGTON, D. C., *March 1936.*

REFERENCES

1. Prandtl, L.: Motions of Fluids with Very Little Viscosity. T. M. No. 452, N. A. C. A., 1928.
2. Blasius, H.: Grenzschichten in Flüssigkeiten mit kleiner Reibung. Z. f. Math. u. Phys., Band 56, Nr. 1, 1908, S. 1–37.
3. van der Hegge Zijnen, B. G.: Measurements of the Velocity Distribution in the Boundary Layer along a Plane Surface. Report 6, Aero. Lab. Tech. H. S., Delft, 1924.
4. Hansen, M.: Velocity Distribution in the Boundary Layer of a Submerged Plate. T. M. No. 585, N. A. C. A., 1930.
5. Éliás, Franz: The Transference of Heat from a Hot Plate to an Air Stream. T. M. No. 614, N. A. C. A., 1931.
6. von Kármán, Th.: Turbulence and Skin Friction. Jour. Aero. Sci., January 1934, pp. 1–20.
7. Dryden, H. L., and Kuethe, A. M.: The Measurement of Fluctuations of Air Speed by the Hot-Wire Anemometer. T. R. No. 320, N. A. C. A., 1929.
8. Runge, C., and Kŏnig, H.: Numerisches Rechnen. Julius Springer (Berlin), 1924, p. 311.
9. Pohlhausen, K.: Zur näherungsweisen Integration der Differentialgleichung der laminaren Grenschicht. Z. f. a. M. M., Band I, Nr. 4, 1921, S. 252.
10. Falkner, V. M., and Skan, Sylvia W.: Some Approximate Solutions of the Boundary Layer Equations. R. & M. No. 1314, British A. R. C., 1930.
11. Dryden, Hugh L.: Computation of the Two-Dimensional Flow in a Laminar Boundary Layer. T. R. No. 497, N. A. C. A., 1934.
12. von Kármán, Th., and Millikan, C. B.: On the Theory of Laminar Boundary Layers Involving Separation. T. R. No. 504, N. A. C. A., 1934.
13. Tollmien, W.: The Production of Turbulence. T. M. No. 609, N. A. C. A., 1931.
14. Schlichting, H.: Zur Entstehung der Turbulenz bei der Plattenströmung. Nach. Gesell. d. Wiss. z. Gött. M. P. K., 1933, S. 181.
15. Tollmien, W.: General Instability Criterion of Laminar Velocity Distribution. T. M. No. 792, N. A. C. A., 1936.
16. Nikuradse, J.: Experimentelle Untersuchungen zur Turbulenzentstehung. Z. f. a. M. M., Band 13, 1933, S. 174.
17. Dryden, Hugh L.: Reduction of Turbulence in Wind Tunnels. T. R. No. 392, N. A. C. A., 1931.
18. Dryden, H. L., and Kuethe, A. M.: Effect of Turbulence in Wind Tunnel Measurements. T. R. No. 342, N. A. C. A., 1930.
19. Mock, W. C., Jr., and Dryden, H. L.: Improved Apparatus for the Measurement of Fluctuations of Air Speed in Turbulent Flow. T. R. No. 448, N. A. C. A., 1932.
20. Piercy, N. A. V., and Richardson, E. G.: On the Flow of Air Adjacent to the Surface of an Aerofoil. R. & M. No. 1224, British A. R. C., 1928.
21. Schubauer, G. B.: Air Flow in a Separating Laminar Boundary Layer. T. R. No. 527, N. A. C. A., 1935.
22. Tollmien, W.: Über die Korrelation der Geschwindigkeitskomponenten in periodisch schwankenden Wirbelverteilungen. Z. f. a. M. M., Band 15, 1935, S. 96.
23. Schlichting, H.: Amplitudenverteilung und Energiebilanz der kleinen Störungen bei der Plattenströmung. Nach. Gesell. d. Wiss. z. Gött., M. P. K., Band I, 1935, S. 47.

TABLE I

SOLUTION OF BLASIUS EQUATION FOR FLOW IN A LAMINAR BOUNDARY LAYER

X	Z	$\frac{dZ}{dX}$	$\frac{d^2Z}{dX^2}$	$\frac{d^3Z}{dX^3}$	$\eta=y\sqrt{\frac{U_0}{\nu x}}$	$\frac{u}{U_0}=\bar{u}$	$\frac{d\bar{u}}{d\eta}$	$\frac{d^2\bar{u}^2}{d\eta^2}$
0	0	0	1	0	0	0	0.3320	0
0.1	0.00500	0.10000	0.99983	−0.00500	0.1819	0.0604	.3320	−0.0009
.2	.02000	.19993	.99867	−.01997	.3639	.1208	.3316	−.0036
.3	.04498	.29966	.99551	−.04478	.5458	.1812	.3306	−.0082
.4	.07992	.39894	.98939	−.07907	.7278	.2410	.3285	−.0144
.5	.12474	.49741	.97940	−.12217	.9097	.3005	.3252	−.0223
.6	.17936	.59466	.96470	−.17303	1.0917	.3593	.3203	−.0316
.7	.24362	.69017	.94459	−.23012	1.2736	.4170	.3137	−.0420
.8	.31732	.78338	.91853	−.29147	1.4556	.4733	.3060	−.0532
.9	.40020	.87367	.88623	−.35467	1.6375	.5278	.2943	−.0647
1.0	.49193	.96042	.84763	−.41698	1.8194	.5803	.2815	−.0761
1.1	.59214	1.04299	.80296	−.47547	2.0014	.6301	.2666	−.0868
1.2	.70037	1.12082	.75276	−.52721	2.1833	.6772	.2500	−.0962
1.3	.81613	1.19339	.69784	−.56952	2.3653	.7210	.2317	−.1039
1.4	.93886	1.26027	.63925	−.60016	2.5472	.7614	.2123	−.1095
1.5	1.06798	1.32116	.57825	−.61756	2.7292	.7982	.1920	−.1127
1.6	1.20289	1.37588	.51620	−.62093	2.9111	.8313	.1714	−.1133
1.7	1.34295	1.42441	.45452	−.61040	3.0931	.8606	.1509	−.1114
1.8	1.48757	1.46684	.39456	−.58693	3.2750	.8862	.1310	−.1071
1.9	1.63613	1.50342	.33751	−.55221	3.4569	.9083	.1121	−.1008
2.0	1.78807	1.53443	.28441	−.50855	3.6389	.9271	.0944	−.0928
2.1	1.94285	1.56046	.23602	−.45855	3.8208	.9428	.0784	−.0837
2.2	2.10001	1.58185	.19282	−.40492	4.0028	.9557	.0640	−.0739
2.3	2.25909	1.59920	.15506	−.35029	4.1847	.9662	.0515	−.0639
2.4	2.41973	1.61305	.12272	−.29694	4.3667	.9745	.0408	−.0542
2.5	2.58160	1.62392	.09557	−.24672	4.5486	.9811	.0317	−.0450
2.6	2.74443	1.63232	.07323	−.20096	4.7305	.9862	.0243	−.0367
2.7	2.90800	1.63871	.05520	−.16052	4.9125	.9900	.0183	−.0293
2.8	3.07212	1.64348	.04093	−.12575	5.0944	.9929	.0136	−.0230
2.9	3.23665	1.64700	.02986	−.09665	5.2764	.9951	.0099	−.0176
3.0	3.40149	1.64954	.02143	−.07289	5.4583	.9966	.0071	−.0133
3.1	3.56654	1.65135	.01513	−.05394	5.6403	.9977	.0050	−.0098
3.2	3.73174	1.65262	.01050	−.03919	5.8222	.9985	.0035	−.0072
3.3	3.89705	1.65350	.00717	−.02795	6.0042	.9990	.0024	−.0051
3.4	4.06243	1.65409	.00482	−.01957	6.1861	.9993	.0016	−.0036
3.5	4.22786	1.65448	.00318	−.01346	6.3680	.9996	.0011	−.0025
3.6	4.39332	1.65474	.00207	−.00909	6.5500	.9997	.0007	−.0017
3.7	4.55881	1.65491	.00132	−.00603	6.7319	.9998	.0004	−.0011
3.8	4.72430	1.65502	.00083	−.00393	6.9139	.9999	.0003	−.0007
3.9	4.88981	1.65508	.00051	−.00251	7.0958	.9999	.0002	−.0005
4.0	5.05532	1.65512	.00031	−.00158	7.2778	1.0000	.0001	−.0003
4.1	5.22083	1.65515	.00019	−.00097	7.4597	----------	.0001	−.0002
4.2	5.38635	1.65516	.00011	−.00059	7.6417	----------	0	−.0001
4.3	5.55187	1.65517	.00006	−.00035	----------	----------	----------	−.0001
4.4	5.71738	1.65518	.00004	−.00021	8.0055	----------	----------	0
4.5	5.88290	1.65518	.00002	−.00012	8.1875	----------	----------	----------
5.2	7.04153	1.65518	0	0	9.4611	----------	----------	----------

TABLE II

CALIBRATIONS OF WIRE N18 ON OCT. 14, 1930

	Beginning	End
Resistance of wire and leads, $R+R_s$, ohms	5.388	5.405
Resistance of leads, R_s, ohms	.445	.446
Resistance of wire, R_0, ohms	4.943	4.959
Temperature, °C	29.0	29.6
Barometric pressure, in Hg	29.68	29.68

Heating current 0.2 ampere. $R_{0\alpha}=0.01653$.

Temperature °C	Speed, u ft./sec.	$\sqrt{u}$	Voltage drop $i(R+R_s)$	$R+R_s$ ohms	R ohms	R_0 ohms	$\frac{i^2RR_{0\alpha}}{R-R_0}$
FIRST CALIBRATION							
28.5	56.6	7.52	1.638	8.190	7.745	4.933	0.001820
	64.5	8.02	1.602	8.010	7.565	----------	.001898
29.0	75.7	8.70	1.561	7.805	7.360	4.943	.002013
	82.7	9.09	1.538	7.690	7.245	----------	.002080
29.0	90.6	9.51	1.520	7.600	7.155	----------	.002138
	100.6	10.03	1.496	7.480	7.035	----------	.002221
29.0	113.9	10.66	1.474	7.370	6.925	----------	.002310
SECOND CALIBRATION							
30.0	105.2	10.25	1.492	7.460	7.014	4.967	0.002267
	100.1	10.05	1.505	7.525	7.079	----------	.002213
30.0	90.8	9.52	1.526	7.630	7.184	----------	.002143
	82.8	9.10	1.546	7.730	7.284	----------	.002080
30.0	71.3	8.44	1.583	7.915	7.469	----------	.001972
	58.2	7.62	1.637	8.185	7.739	----------	.001845

TABLE III

DETERMINATION OF MEAN SPEED FOR $x=23$ INCHES, $U_0=105.2$ FT./SEC. ON OCT. 14, 1930

SEE TABLE II FOR DATA ON WIRE. SEE FIGURE 7 FOR CALIBRATION CURVE

Temperature °C	y inches	Voltage drop $i(R+R_s)$	$R+R_s$ ohms	R ohms	R_0 ohms	$\frac{i^2RR_{0\alpha}}{R-R_0}$	$\sqrt{u}$	u ft./sec.	$\frac{u}{U_0}$
29	0.015	1.862	9.310	8.865	4.943	0.001494	5.42	29.4	0.280
29.5	.020	1.785	8.825	8.379	4.954	.001616	6.19	38.3	.364
29.5	.025	1.720	8.600	8.154	-------	.001634	6.62	43.8	.417
29.5	.030	1.666	8.330	7.884	-------	.001778	7.21	52.0	.494
30.0	.040	1.602	8.010	7.565	4.967	.001926	8.15	66.4	.632
30.0	.050	1.566	7.830	7.384	-------	.002021	8.75	76.5	.728
30.0	.065	1.529	7.645	7.199	-------	.002130	9.45	89.2	.848
30.0	.080	1.508	7.540	7.096	-------	.002203	9.91	98.3	.935
30.0	.100	1.499	7.495	7.049	-------	.002237	10.13	102.6	.976
30.0	.130	1.493	7.465	7.019	-------	.002259	10.26	105.3	1.001
30.0	.180	1.490	7.450	7.004	-------	.002274	10.36	107.6	1.024
30.0	.230	1.490	7.450	7.004	-------	.002274	10.36	107.6	1.024
30.0	1.065	1.493	7.465	7.019	-------	.002259	10.26	105.3	1.001

TABLE IV

RESULTS OF TABLE III CORRECTED FOR HEAT LOSS TO PLATE ON BASIS OF STILL AIR CORRECTION

WIRE LENGTH—0.342 INCH. K=0.000 000 00435

y inches	$\frac{R-R_0}{R_0\alpha}=\theta$ °C.	$\frac{K\theta}{y}$	$\frac{i^2RR_0\alpha}{R-R_0}\frac{K\theta}{y}$	$\sqrt{u_\theta}$	u_θ ft./sec.	$\frac{u_\theta}{U_0}$
0.015	237.2	0.000069	0.001425	4.93	24.3	0.231
.020	207.2	.000045	.001571	5.90	34.8	.331
.025	193.6	.000034	.001650	6.40	41.0	.390
.030	177.2	.000026	.001752	7.06	49.8	.473
.040	157.1	.000017	.001909	8.05	64.8	.616
.050	146.2	.000013	.002008	8.68	75.3	.716
.065	135.1	.000009	.002121	9.38	88.0	.836
.080	128.7	.000007	.002196	9.85	97.0	.922
.100	126.0	.000005	.002232	10.09	101.8	.968
.130	124.1	.000004	.002255	10.25	105.0	.998
.180	123.2	.000003	.002271	10.35	107.5	1.022
.230	123.2	.000002	.002272	10.35	107.5	1.022
1.065	124.1	0	.002259	10.26	105.3	1.001

TABLE V

DETERMINATION OF SPEED FLUCTUATION FOR x=23 INCHES, U_0=105.2 FT./SEC. ON OCT. 14, 1930

SEE TABLE II FOR DATA ON WIRE, TABLE III FOR MEAN SPEED, FIG. 7 FOR CALIBRATION CURVE

B=0.0001580 (from fig. 7)

1	2	3	4	5	6	7	8	9
y inches	$\sqrt{u}$	$\frac{iR_0^2\alpha}{(R-R_0)^2}$	$\frac{i^2RR_0\alpha}{6(R-R_0)}$	(3)+(4)	$\frac{2(5)}{B\sqrt{u}}$	dE (volts)	$\frac{du}{u}$	$\frac{du}{U_0}$
0.015	5.42	0.001061	0.000249	0.001310	3.06	0.1190	0.364	0.1019
.020	6.19	.001396	.000269	.001665	3.40	.0776	.264	.0961
.025	6.62	.001597	.000281	.001878	3.59	.0563	.202	.0843
.030	7.21	.001905	.000296	.002201	3.86	.0403	.1555	.0768
.040	8.15	.002436	.000321	.002757	4.28	.0171	.0732	.0462
.050	8.75	.002812	.000337	.003149	4.56	.0122	.0556	.0405
.065	9.45	.003290	.000355	.003645	4.88	.0099	.0483	.0410
.080	9.91	.003623	.000367	.003990	5.10	.0090	.0459	.0429
.100	10.13	.003780	.000373	.004153	5.19	.00838	.0435	.0425
.130	10.26	.003896	.000376	.004273	5.27	.00582	.0307	.0307
.180	10.36	.003958	.000379	.004337	5.29	.00360	.0191	.0196
.230	10.36	.003958	.000379	.004337	5.29	.00266	.0141	.0144
1.065	10.26	.003896	.000376	.004272	5.27	.00115	.0061	.0061

TABLE VI

RESULTS OF TABLE V CORRECTED FOR HEAT LOSS TO PLATE ON BASIS OF STILL AIR CORRECTION

WIRE LENGTH 0.342 INCHES K=0.000 000 00435

1	2	3	4	5	6	7	8
y inches	$\sqrt{u_\theta}$	$\frac{K}{y\,iR_0\alpha}$	Column (5) of table V +(3)	$\frac{2(4)}{B\sqrt{u_\theta}}$	dE volts	$\frac{du_\theta}{u_\theta}$	$\frac{du_\theta}{U_0}$
0.015	4.93	0.000088	0.001398	3.59	0.1190	0.427	0.0936
.020	5.90	.000066	.001731	3.72	.0776	.289	.0957
.025	6.40	.000053	.001931	3.82	.0563	.215	.0838
.030	7.06	.000044	.002245	4.03	.0403	.1612	.0763
.040	8.05	.000033	.002790	4.39	.0171	.0751	.0463
.050	8.68	.000026	.003175	4.63	.0122	.0565	.0404
.065	9.38	.000020	.003665	4.95	.0099	.0490	.0410
.080	9.85	.000016	.004006	5.15	.0090	.0403	.0427
.100	10.09	.000013	.004166	5.23	.00838	.0433	.0424
.130	10.25	.000010	.004282	5.29	.00582	.0308	.0307
.180	10.35	.000007	.004344	5.31	.00360	.0191	.0195
.230	10.35	.000006	.004343	5.31	.00266	.0141	.0144
1.065	10.26	.000001	.004273	5.27	.00115	.0061	.0061

TABLE VII

FAIRED VALUES FOR x=23 INCHES, U_0=105.2 FT./SEC.

Average temperature 30° C. Pressure 29.68 inches Hg

ν=0.0001732 ft²/sec. $\frac{U_0x}{\nu}$=1,164,000

$\frac{u}{U_0}$	y inch	$\frac{U_0y}{\nu}$	$100\frac{du}{U_0}$	y	$\frac{U_0y}{\nu}$
0.3	0.0166	841	10	0.0166	841
.4	.0230	1,165	9	.0237	1,200
.5	.0301	1,525	8	.0282	1,428
.6	.0378	1,915	7	.0310	1,570
.7	.0468	2,371	6	.0327	1,656
.8	.0580	2,938	5	.0367	1,859
.9	.0727	3,682	4	.057	2,888
				.110	5,575
			3	.132	6,690
			2	.179	9,070

TABLE VIII

y-REYNOLDS NUMBERS CORRESPONDING TO VARIOUS VALUES OF u-FLUCTUATION USED IN PLOTTING FIGURE 22

$100\frac{du}{U_0}$	x-Reynolds Number											
	102000	256200	507000 [1]	567000	555000	863000	869000	1188000	1160000	1164000	1390000	1283000
11											490 1130	1270
10.5									960 1560		1230	1330
10.0									890 1590	760	1350	1410
9.5								1330	880 1630	1030	1470	1510
9.0								1480	790 1660	1160	1580	1610
8.5								1620	1700	1280	1700	1730
8.0								1770	1730	1420	1830	1880
7.5								1920	1800	1570	1970	2020
7.0								2060	1890	1660	2120	2220
6.5								2270	2000	1750	2290	2450
6.0								2500	2150	1820	2470	2770 3200 5440
5.5								2820	2300	1910	2680 3740 5900	5960
5.0			1080 1390					3250	2620	1980	6410	6420
4.5			770 1510					3670	2990 4390	2090	6950	6940
4.0			1870					4180	5400	5570	7640	7560
3.5			2000					4960	5860	6080	8480	8360
3.0			2140			1010 1530 1900	1190 1470		6360	6690	9320	9090
2.5	780 330		2320			1170 1330 2010	1860		7170	7770	10100	10050
2.0	1000		2570		1260	2990	3100			9070	11920	11160
1.5	1190	1380	2830	1060 2560	510 2440	4120	3800			11250	12760	12350
1.0	1380	1880	3270	3170	3200	4650	4590				13550	13630

[1] Not considered, because not concordant with repeat runs.

TABLE IX

y-REYNOLDS NUMBERS CORRESPONDING TO VARIOUS VALUES OF u-FLUCTUATION USED IN PLOTTING FIGURE 26

U_0=32.6 ft./sec.

$100\frac{du}{U_0}$	x-Reynolds Number							
	62800	123400	156100	186400	215300	251200	439500	437300
8.0			255 435					
7.5			210 490	270 455				
7.0			190 560	240 500	240 385			
6.5		300 450	165 645	205 570	175 460			
6.0		255 535	155 770	190 670	170 495			
				1505 2105	1660 2355			
5.5		215 865 1740	1090 1560	160 810 1300 2525	160 505 915 2695	310 460 1040 2830		
5.0		170 2070	2475	155 1025 1125 2835	155 3220	230 580 880 3450		
4.5		2360	2730	3265	3695	190 4100	1995 6080	1780 5810
4.0	630 1180	2700	2940	3835	4540	150 4770	785 7535	335 7060
3.5	475 1515	3135	3330	4700	5545	5540	11450	225 9210
3.0	375							185

U_0=65.5 ft/sec.

$100\frac{du}{U_0}$	x-Reynolds Number:											
	63000	125200	156000	188500	217300	252200	307500	352000	406000	558000	716000	888000
7.5				380	250 355							
7.0			265 395	460	425							
6.5			435	530	500							
6.0			500 1390 2180	595 1400 2390	575 1555 2715	2095 2400						
5.5		470 1385 1720	560 1185 1810	660 1200 2710	645 1335 3075	355 485 1545 2360	1750 3170	2875 3245				
5.0		550 1165 2110	640 960 2775	715 975 3080	800 1135 3540	335 585 1290 3650	400 1355 3585	1620 4375				8250 12140
4.5	670 1560	650 960 2380	3230	3640	4160	320 4550	540 1005 5065	260 1185 5260	3305 4930	6195	4790 11470	4795 13700
4.0	2060	2850	4055	4555	5070	6000	6070	6710	1695 7490	2540 12570	2070 14980	995 15380
3.5		3960	5550	9430	6390		7940	8960	10730	1395 14340	20680	305 10020